Strategic Planning, Design, and Development of the Shale Gas Supply Chain Network

Diego C. Cafaro
INTEC (UNL–CONICET), Güemes 3450, Santa Fe 3000, Argentina

Ignacio E. Grossmann
Dept. of Chemical Engineering, Carnegie Mellon University, Pittsburgh, PA15213

DOI 10.1002/aic.14405
Published online March 1, 2014 in Wiley Online Library (wileyonlinelibrary.com)

The long-term planning of the shale gas supply chain is a relevant problem that has not been addressed before in the literature. This article presents a mixed-integer nonlinear programming (MINLP) model to optimally determine the number of wells to drill at every location, the size of gas processing plants, the section and length of pipelines for gathering raw gas and delivering processed gas and by-products, the power of gas compressors, and the amount of freshwater required from reservoirs for drilling and hydraulic fracturing so as to maximize the net present value of the project. Because the proposed model is a large-scale nonconvex MINLP, we develop a decomposition approach based on successively refining a piecewise linear approximation of the objective function. Results on realistic instances show the importance of heavier hydrocarbons to the economics of the project, as well as the optimal usage of the infrastructure by properly planning the drilling strategy. © 2014 American Institute of Chemical Engineers *AIChE J*, 60: 2122–2142, 2014

Keywords: shale gas, supply chain, strategic plan, mixed-integer nonlinear programming approach, solution algorithm

Introduction

Natural gas is an abundant energy source and the cleanest-burning fossil fuel. Natural gas extracted from dense shale rock formations has become the fastest-growing fuel in the United States and could become a significant new global energy source. Over the past decade, the combination of horizontal drilling and hydraulic fracturing has allowed access to large volumes of shale gas that were previously uneconomical to produce. The production of natural gas from shale formations has reinvigorated the natural gas and chemical industries in the United States. The Energy Information Administration projects U.S. shale gas production to grow from 23% to almost 50% of the total gas production in the next 25 years.[1] Shale gas is found in plays containing significant accumulations of natural gas, sharing similar geologic and geographic properties. A decade of production has come from the Barnett Shale play in Texas. Experience gained from Barnett Shale has improved the efficiency of shale gas development around the country. Today, one of the most productive plays is the Marcellus Shale in the eastern U.S., mainly in Pennsylvania. Regarding both economic and environmental impacts, the long-term planning and development of the shale gas supply chain network around each play is a very relevant problem. However, to the best of our knowledge, it has not been addressed before in the literature.

Correspondence concerning this article should be addressed to I. E. Grossmann at grossmann@cmu.edu.

The raw gas extracted from shale formations is transported from wellbores to processing plants through pipelines. The processing of shale gas consists of the separation of the various hydrocarbons and fluids from the pure gas (methane) to produce what is known as "pipeline quality" dry natural gas.[2] This means that before the natural gas can be transported by midstream distributors, it must be purified to meet the requirement for pipeline, industrial, and commercial uses. The associated hydrocarbons (ethane, propane, butane, pentanes, and natural gasoline) known as natural gas liquids (NGLs) are valuable byproducts after the natural gas has been purified and fractionated. These NGLs are sold separately (usually through dedicated pipelines) and have a variety of different uses, including enhancing oil recovery in wells, providing raw materials for oil refineries or petrochemical plants, and as sources of energy.[3] One of the most critical issues in the design and planning of the shale gas supply chain network is the sizing and location of new shale gas processing and fractionation plants (as well as future expansions) due to their high cost.

In addition, the number of wells drilled in each location can dramatically influence costs and the ecological footprint of natural gas operations.[4] The ability to drill multiple wells from a single location (or "pad") is seen as a major technological breakthrough driving natural gas development as for instance has happened in the Marcellus Shale. The utilization of multiwell pads also has large environmental and socioeconomic implications given that as many as 20 or more natural gas wells and associated pipeline infrastructure can be concentrated in a single location. Furthermore, the total amount

of industrial activity can be compressed as these wells can be drilled in rapid-succession and the technology now exists to perform hydraulic fracturing stimulations on multiple wells simultaneously. Hence, another key decision tackled by this article is the drilling strategy, that is, how many wells to set up or add on existing well-pads at every period.

Another critical aspect in the shale gas production is water management. Shale gas production is a highly water-intensive process, with a typical well requiring around 20,000 m^3 of water normally over a 3-month period to drill and fracture, depending on the basin and geological formation.[5] The vast majority of this water is used during the fracturing process, with large volumes of water pumped into the well with sand and chemicals to facilitate the extraction of the gas. Although increasing amounts of water are being recycled and reused, freshwater is still required in large quantities for the drilling operations as flowback water usually only represents about 25–30% of the water injected into the well. Despite the overall use of water for well fracturing, it represents less than 1% of the total water consumption in the United States (with irrigation and thermal power generation each accounting for about 40%). However, the need for freshwater is an issue of growing importance, especially in water-scarce regions and in areas with high cumulative demand for water, leading to pressure on sources and competition for water withdrawal permits. Therefore, a long-term planning model for the development of shale gas fields should also account for water availability.

The goal of this article is to develop a mixed-integer nonlinear programming (MINLP) model for the sustainable long-term planning and development of shale gas supply chains, which should optimally determine: (a) the number of wells to drill on new/existing pads; (b) the size and location of new gas processing plants (as well as future expansions); (c) the section, length, and location of new pipelines for gathering raw gas, delivering dry gas, and moving NGLs; (d) the location and power of new gas compressors to be installed, according to the flow rate at every line; and (e) the amount of freshwater coming from available reservoirs used for well drilling and fracturing so as to maximize the economic results (net present value or NPV) over a planning horizon comprising 10 years.

Literature review

Foundational papers in the optimal design and planning of supply chains were published in the literature 40 years ago.[6] A complete review on more recent developments in supply chain optimization problems can be found in the work of Melo et al.[7] Regarding the strategic planning of natural gas supply chains, Durán and Grossmann[8] propose a superstructure representation, an MINLP model and a solution strategy for the optimal synthesis of gas pipelines, deciding on the gathering pipeline system configuration, compressors power, and pipeline pressures. Iyer et al.[9] propose a multiperiod mixed-integer linear programming (MILP) model for the optimal planning and scheduling of offshore oilfield infrastructure investment and operations. As the resulting model becomes intractable due to the large-scale, nonlinear reservoir equations are approximated through piecewise linear functions and a sequential decomposition strategy is used. Van den Heever and Grossmann[10] propose a multiperiod generalized nonlinear disjunctive programming model for oilfield infrastructure planning, whose optimal solution is found through a bilevel decomposition method. In this model, the number of wells is given beforehand through a fixed drilling plan. More recently, Gupta and Grossmann[11] address some new features of the same problem, accounting for all three components (oil, water, and gas) explicitly in the formulation. They also incorporate more accurate estimations of the nonlinear reservoir behavior, variable number of wells for each field (to capture drill rig limitations), and facility expansions, including their lead times.

Conversely, some work has also been reported on the optimization of the operation of shale gas fields. Rahman et al.[12] present an integrated optimization model for hydraulic fracturing design, accounting for fracture geometry, material balances, operational limitations, characteristics of the gas formation, and production profiles. By combining genetic algorithms and evolutionary techniques, improved hydraulic fracturing designs permit to reduce the treatment (stimulation) costs up to 44% at the expense of a 12% reduction in the gas production. Knudsen et al. (submitted for publication) propose a Lagrangian relaxation-based approach for scheduling shut-ins times in tight formation multiwell pads to stimulate the shale gas production in different wells to comply with the gas rates required by the distribution company. In that work, a proxy model captures the physics during shut-in operations. Based on the proxy model results, the time domain is discretized into daily periods, and an MILP model is then solved using Lagrangian relaxation techniques.

Finally, few recent publications deal with the strategic and operational management of water resources and other environmental concerns in the development of shale gas plays. Mauter et al.[13] argue that strategic planning by both companies and regulatory agencies is critical to mitigate the environmental impacts of unconventional extraction. Rahm and Riha[14] attempt to determine water resource impacts of shale gas extraction, from regional, collective-based perspectives, seeking to balance the need for development with environmental concerns and regulatory constraints. Yang and Grossmann[15] present an MILP formulation whose main objective is to schedule the drilling and fracturing at well-pads to minimize the transportation, treatment, and freshwater acquisition costs, as well as treatment infrastructure, while maximizing the number of well stages to be completed within the specified time horizon. The goal is to find an optimal short-term fracturing schedule, the water recycling ratio, and the need for additional impoundment and treatment capacity.

Like most enterprise-wide optimization (EWO) problems, the strategic planning of the shale gas supply chain has great economic potential. Considerable effort has been spent toward the solution of EWO problems during the last 20 years, particularly in the field of oil and gas production.[16] But none of them has been focused on the shale gas supply chain. The shale gas production has its own peculiarities, and is a problem of very recent development.[17] In fact, one of the major barriers is the size and complexity of computational optimization models for achieving the goal of EWO.[18] The strategic planning of shale gas infrastructure consists on the design of large supply chains, including well-pads, processing plants, compressors, product delivery nodes, and the complex pipeline network transporting shale gas and the resulting hydrocarbons. As concluded by Oliveira et al.,[19] careful evaluation of the investment options in this kind of problems has particular importance, and the use of efficient decision-making tools that capture the problem complexity becomes crucial.

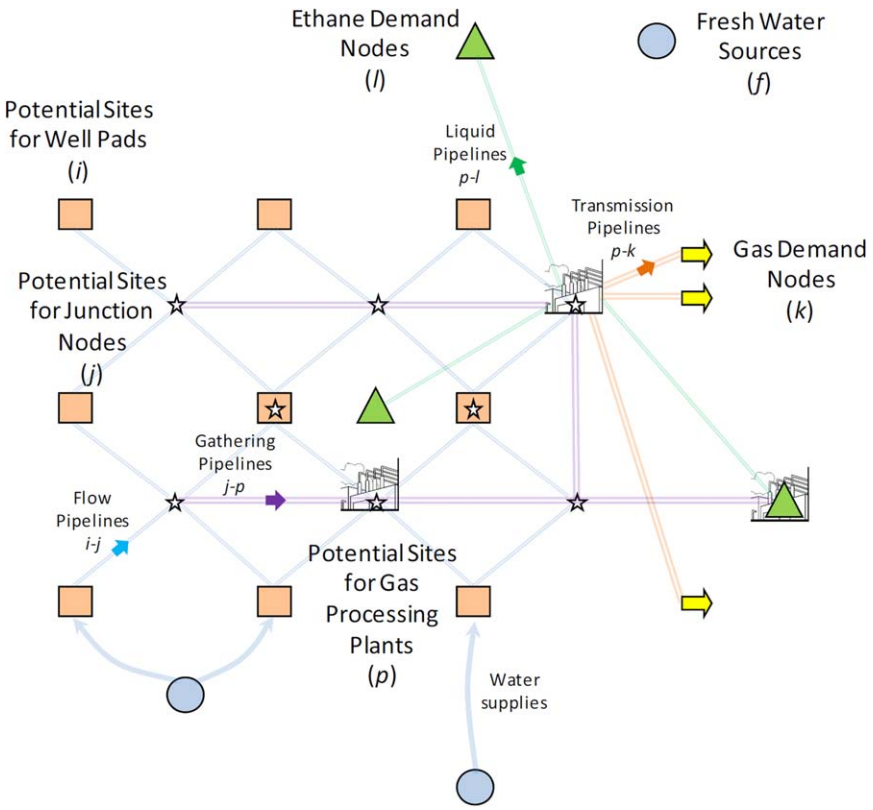

Figure 1. A simplified superstructure of the shale gas supply chain (for the sake of clarity, only few arcs of each type are drawn).

[Color figure can be viewed in the online issue, which is available at wileyonlinelibrary.com.]

Problem Description

We address the problem of determining the optimal design for a shale gas supply chain network, the well drilling, and hydraulic fracturing strategy over the planning horizon, together with the size and location of gas separation plants, compressors, and pipeline infrastructure, in order to maximize the NPV of the project. This problem can be formally stated as follows.

A comprehensive shale gas supply chain network superstructure like the one depicted in Figure 1 is given. It includes: (a) potential or existing well-pads where new wells can be drilled and hydraulically fractured over the planning horizon (nodes $i \in I$), (b) possible or existing junction nodes where shale gas flows coming from nearby well-pads converge (nodes $j \in J$), (c) potential or existing flow pipelines connecting nodes i and j, (d) possible sites for the installation/expansion of new/existing shale gas processing plants (nodes $p \in P$), (e) potential/existing gathering pipelines connecting junction nodes j with plant sites p, (f) demand nodes for dry natural gas (nodes $k \in K$) and ethane (nodes $l \in L$), (g) possible/existing transmission and liquid pipelines connecting plant sites p with nodes k and l, respectively, and (h) freshwater source nodes from where the water required for drilling and fracturing new wells can be supplied.

A strategic long-term planning horizon is considered. In this article, a planning horizon of 10 years is divided into 40 time periods (quarters). The reasons for this time discretization are as follows: (1) Gas prices normally exhibit a seasonal behavior with a high peak in the winter. (2) The drilling and completion of wells normally takes between 50 and 90 days, plus the following 20 days during which the well does not produce a steady stream of gas, but a flowback of water that is captured and stored for further treatment. Overall, approximately 90 days (3 months) are required since the well-pad is set up and wells start to be drilled until they begin to produce a steady flow of shale gas. (3) Freshwater availability in some water-scarce regions is strongly seasonal, and can be a critical issue if high cumulative demand for water leads to pressure on sources and competition for water withdrawal permits.

Besides the network superstructure and the time horizon, the productivity profile of every well at any location is assumed to be deterministic and known beforehand. Dry and semidry shale gas wells exhibit many of the same characteristics: an early peak in the gas rate from the sudden release of gas stored in pores and natural fracture networks, followed by a long transient decline in the production rate. Such decline in the rate is caused both by pressure loss and the inherently low permeability of shale rocks. In this problem, the well productivity is represented by a discrete-time decreasing function of the well age. The parameter $pw_{i,\tau}$ stands for the average production rate of a shale gas well of age τ (given in quarters) drilled in location i (see Figure 2). As recently proposed by Patzek et al.,[20] the long-term gas production from shale can be predicted by a simple scaling theory, showing two regimes. In the early-time regime, recovery rate declines with the square root of time, and in the late-time regime, production decreases exponentially. This diffusion-type model is based on several parameters: the number of hydrofracture stages, the half-distance between hydrofractures, the hydraulic diffusivity (proportional to the permeability of the rock and inversely

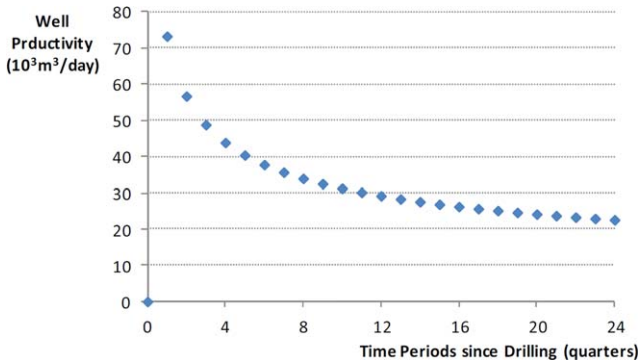

Figure 2. Discrete-time well productivity profile.

[Color figure can be viewed in the online issue, which is available at wileyonlinelibrary.com.]

proportional to the gas viscosity and compressibility), and the total amount of gas that can ultimately be recovered. In summary, either from experimental, theoretical, or computational analysis, the long-term forecast of gas production at every well-pad is given data for the optimization model.

Moreover, the shale gas composition, and particularly its "wetness" (% of hydrocarbons others than methane), are assumed to be known and independent of both the well site and its age. Relaxing this assumption is discussed later in this article.

Regarding the pipeline infrastructure, gas and liquid pipelines must be considered separately. On the one hand, gas pipelines (transporting either raw or processed gas) are assumed to handle an ideal mixture of ideal gases. Raw gas pipelines connecting nodes i to j (well-pads to junction nodes) and j to p (junction nodes to plants) operate at medium–low pressures, whereas transmission pipelines p-k supplying gas demand nodes from processing plants operate at higher pressures. For simplicity, gas suction/discharge pressures (measured in MPa) at every node of the network are assumed to be given constant values. These are as follows: (1) shale gas discharge pressure at the well-pads is Pd_i, (2) junction nodes receive the shale gas at a pressure of $\mathrm{Ps}_j < \mathrm{Pd}_i$, (3) compressor stations installed at junction nodes increase the pressure from Ps_j to Pd_j, to make the gas flow toward processing plants, (4) the shale gas pressure at the inlet of processing plants is $\mathrm{Pi}_p < \mathrm{Pd}_j$, (5) processing plants deliver dry gas at a pressure of Po_p, (6) compressor stations installed at the outlet of processing plants increase the dry gas pressure from $\mathrm{Po}_p = \mathrm{Ps}_p$ to Pd_p before sending flows to markets, and (7) gas demand nodes receive dry gas at a pressure of $\mathrm{Pr}_k < \mathrm{Pd}_p$. By fixing such values, the maximum flow of a gas pipeline is directly proportional to the pipeline diameter raised to the power of 2.667, and the proportionality factor depends on the gas properties, the input/output pressures and the pipeline length.[8,21] Moreover, compressors are assumed to be adiabatic and their power (measured in kW) is directly proportional to the gas flow, as the compression ratio is a given parameter. More details are given in Appendix A.

Conversely, liquid pipelines transport hydrocarbons like ethane, propane, butane, pentanes, and natural gasoline (NGLs) in liquid state from separation plants to either petrochemical plants or liquefied petroleum gases (LPGs) distribution facilities. In this problem, all NGLs except ethane are assumed to be separately sold to customers near the processing plants, whereas ethane is continuously delivered to petrochemical plants by dedicated pipelines. The maximum flow in liquid pipelines is assumed to be directly proportional to the pipeline section as a maximum mean velocity is imposed (typically, 1.5 m/s).

An illustrative example comparing two network designs is presented in Figure 3. The shale gas produced at two different well-pads $i1$ and $i2$ is sent to a processing plant in two alternative ways: (A) through an intermediate junction node $j1$, or (B) directly, through separate lines. Typical values for the suction and discharge pressures at each node are given in the figure. The example also reveals one of the trade-offs to be determined by the model. Option (A) requires a compressor station at node $j1$, but pipelines are smaller in diameter and shorter than in option (B) which does not require a compressor. Pipeline and compressor costs with regards to their size (usually determined by economies of scale functions) are the key to determine which option is the most convenient.

Finally, freshwater consumption, mainly for hydraulic fracturing, is considered to be a fixed volume required during the drilling period, which depends on the well-pad location and the possibility of reusing the flowback water. The selection of optimal sources for water supply is a key model decision, but no details on the water transportation logistics are considered at this planning level. Other operational issues like flowback water capture, treatment and final disposal, as well as planning shut-ins and well stimulations are also out of the scope of this work.

Given all the problem conditions described above, the goal is to optimally determine: (a) the number of wells to

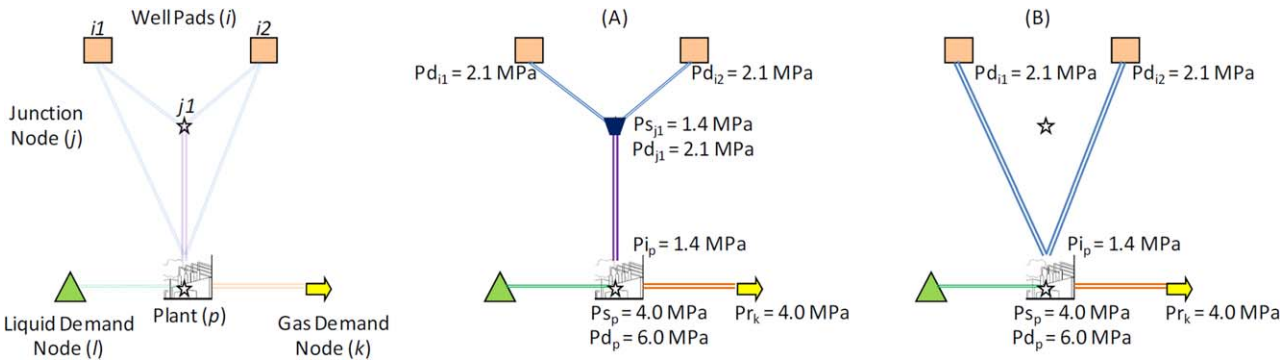

Figure 3. Simplified network superstructure and alternative network designs.

[Color figure can be viewed in the online issue, which is available at wileyonlinelibrary.com.]

drill on new/existing pads at every trimester; (b) the size and location of new gas processing plants (as well as future expansions); (c) the section, length, and location of new pipelines for gathering raw gas, delivering dry gas, and transporting NGLs; (d) the location and power of new gas compressors to be installed; and (e) the amount of freshwater coming from available reservoirs, used for well drilling and fracturing so as to maximize the NPV of the project.

Assumptions

The main assumptions have already been discussed and can be summarized as follows:

1. Shale gas is assumed to be a mixture of ideal gases.
2. The composition, and particularly the shale gas "wetness," are known constants independent of the well location. The relaxation of this assumption is discussed after the model presentation.
3. The planning horizon is discretized in time periods, commonly quarters.
4. Multiple wells can be drilled in a single pad over one time period, although not necessarily at the same time. It is assumed that all of them are hydraulic fractured and completed within the same time period they are drilled.
5. Wells start to produce shale gas in the period following the drilling period. Once the wells are completed, their production cannot be delayed by shutting them in. This assumption can be relaxed as shown in Appendix B.
6. After the well is completed, its productivity rate is a decreasing function of the well age. In other words, a discrete-time function as depicted in Figure 2 is assumed to be known. Given the strategic nature of the problem, the model does not consider other operational decisions on gas production, like midlife stimulations or shut-ins. Such decisions are left to a more detailed planning stage.
7. Multiwell pads can be set up, and multiple wells in the same pad can be drilled, fractured, and completed during the same period. However, an upper bound is given due to technology limitations. Moreover, the total number of wells that can be drilled in the same pad all over the time horizon is also bounded.
8. The pressure at pipelines transporting raw gas from well-pads to junction nodes decreases from Pd_i to Ps_j as a function of their length[20] (for further details see Appendix A). The same is also valid for pipelines transporting raw gas from junction nodes to processing plants (from Pd_j to Pi_p), and dry gas from plants to demand nodes (from Pd_p to Pr_k).
9. All the gas pressures (Pd_i at the outlet of pad i; Ps_j at the inlet of the junction node j; Pd_j at the outlet of j; Pi_p at the inlet of the plant p; $Po_p = Ps_p$ at the outlet of plant p; Pd_p at the outlet of the p-compressor station; and Pr_k at the gas demand node k) are given. Relaxing this assumption would imply solving a much more complex optimization problem.[8] Although pressure optimization is out of the scope for this model, it will be shown later that varying pressure levels within normal values does not lead to major changes in the optimal solution.
10. The liquid pipeline flow is bounded to a maximum mean velocity (commonly1.5 m/s).
11. Centrifugal pumps have a negligible cost compared with processing plants, pipelines, and gas compressors.
12. Shale gas processing plants separate NGLs (namely ethane, propane, butane, pentanes, and natural gasoline) from the shale gas (methane), also capturing H_2S, CO_2, N_2, and H_2O; and finally delivering the methane to consumer markets. All NGLs except ethane are sold to nearby markets, whereas ethane is sent to chemical plants by dedicated pipelines.
13. Concave cost functions of the form $f(x) = c\,x^r$ (with $0 < r < 1$ and $c > 0$) are assumed in the calculation of: (a) the cost $f_a(x_a)$ of a shale gas processing plant with a capacity of $x_a \times 10^6$ m^3/day,[22] (b) the cost $f_b(x_b)$ of a pipeline of diameter x_b, (c) the cost $f_c(x_c)$ of a compressor station of power x_c,[23] and (d) the cost $f_d(x_d)$ of drilling and hydraulically fracturing x_d wells during the same quarter year.
14. Pipeline diameters are treated as continuous variables. To handle gas/liquid flows, it is assumed that diameters are continuous in the model, but after the solution they are rounded up to the closest commercial diameter. A rigorous model would explicitly handle discrete size diameters, but this is out of scope for this work.

Mathematical Formulation

The optimization problem for the long-term planning, design, and development of the shale gas supply chain is formalized in terms of a MINLP model described in the following sections.

Model constraints

The feasible region of the model is determined by a set of linear constraints. They are grouped into five blocks: Shale Gas Production; Flow Balances; Plants, Pipelines and Compressors Sizing; Water Supplies; and Maximum Demands.

Shale Gas Production. ***Number of Wells Drilled in a Pad.*** The number of wells drilled, fractured, and completed in the multiwell pad i during the period t is represented by the variable $N_{i,t}$. Its value is determined by Eq. 1 in terms of 0–1 variables $y_{i,n,t}$, one of which is equal to one to make $N_{i,t} = n$. The index n stands for an integer number greater or equal to zero and less or equal to $\check{n}_i$, where $\check{n}_i$ is the maximum number of wells that can be drilled during a single quarter in pad i. For the examples solved in the results section, the value of $\check{n}_i$ varies from 2 to 4. Moreover, the total number of wells that can be drilled in a pad all over the planning horizon is bounded by Eq. 3 to a maximum of $\check{N}_i$. The current trend in shale gas production is to increase this number as much as possible to reduce the environmental impact[4]

$$N_{i,t} = \sum_{n=0}^{\check{n}_i} n\, y_{i,n,t} \quad \forall i \in I, t \in T \tag{1}$$

$$\sum_{n=0}^{\check{n}_i} y_{i,n,t} = 1 \quad \forall i \in I, t \in T \tag{2}$$

$$\sum_{t \in T} N_{i,t} \le \check{N}_i \quad \forall i \in I \tag{3}$$

Shale Gas Production at Every Well-Pad. As stated in the model assumptions, the total production of shale gas (including methane, ethane, and other NGLs) in a well-pad i

at a certain period t depends on the age of every active well at that time. If $pw_{i,a}$ is a model parameter standing for the productivity of a well drilled in pad i, a quarters before the current time period t, then the total daily production coming from all the wells in pad i can be determined through Eq. 4. Note that at time t, the age of a well drilled in time period $\tau < t$ is $a = t - \tau$. Moreover, wells of age "0" (being drilled and fractured) do not produce gas until the following period (see Figure 2)

$$\sum_{\tau=1}^{t-1} N_{i,\tau} pw_{i,t-\tau} = SP_{i,t} \quad \forall i \in I, t > 1 \tag{4}$$

Methane, Ethane, and other NGLs Produced at Well-Pads. As the shale gas composition at every well is assumed to be the same (uniform gas "wetness"), the production of such fuels within the shale gas stream coming from each well-pad can be easily determined by Eqs. 5–7

$$SP^{G}_{i,t} = gc\, SP_{i,t} \quad \forall i \in I, t > 1 \tag{5}$$

$$SP^{E}_{i,t} = ec\, SP_{i,t} \quad \forall i \in I, t > 1 \tag{6}$$

$$SP^{L}_{i,t} = lc\, SP_{i,t} \quad \forall i \in I, t > 1 \tag{7}$$

where "gc" is the volume methane composition, "ec" is the ethane composition, and "lc" is the remaining hydrocarbons composition. If these parameters become dependent on the well location, the model structure must be modified to preserve the linearity of model constraints. This will be discussed in a further section.

Flow Balances. Stream Flows from a Well-Pad to Junction Nodes. Shale gas production at a certain pad during a time period is sent to one or more junction nodes (depending on the network design), which is controlled by Eq. 8

$$SP_{i,t} = \sum_{j \in J} FP_{i,j,t} \quad \forall i \in I, t > 1 \tag{8}$$

The model variable $FP_{i,j,t}$ stands for the daily shale gas flowing from pad i to junction node j during period t. By simple extension of Eqs. 5–7, individual hydrocarbon flows in the shale gas stream ($FP^{G}_{i,j,t}$, $FP^{E}_{i,j,t}$, and $FP^{L}_{i,j,t}$) can be easily obtained.

Flow Balances at Junction Nodes. Equation 9 states that the sum of incoming shale gas flows at a certain junction node equals the sum of outgoing streams sent to one or more processing plants, depending on the network design. Under the given assumptions, flow splitting at well-pads and junction nodes are both allowed

$$\sum_{i \in I} FP_{i,j,t} = \sum_{p \in P} GP_{j,p,t} \quad \forall j \in J, t > 1 \tag{9}$$

Similarly to variable $FP_{i,j,t}$, individual fuel flows can also be derived from the shale gas stream flowing between nodes j and p ($GP_{j,p,t}$, $GP^{G}_{j,p,t}$, $GP^{E}_{j,p,t}$, and $GP^{L}_{j,p,t}$).

Flow Balances at Separation Plants. Assuming that the total flow of methane converging to processing plant p together with the shale gas stream is separated and sent to one or more dry gas demand nodes k, Eq. 10 is added to the formulation. $TP_{p,k,t}$ is the flow of dry gas transported through pipeline p-k during period t

$$\sum_{j \in J} GP^{G}_{j,p,t} = \sum_{k \in K} TP_{p,k,t} \quad \forall p \in P, t > 1 \tag{10}$$

The same also applies for ethane flows, which are received with the shale gas, separated and pumped to one or more petrochemical plants l in liquid state through dedicated pipelines p-l, at a rate of $LP_{p,l,t}$ tons per day, during the whole period t

$$s^{E}_{g} \sum_{j \in J} GP^{E}_{j,p,t} = \sum_{l \in L} LP_{p,l,t} \quad \forall p \in P, t > 1 \tag{11}$$

s^{E}_{g} is the density of ethane gas in standard conditions, given in ton/10^6 m^3.

Finally, other NGLs are processed and sold to nearby markets at a rate of $NP_{p,t}$ tons per day as stated by Eq. 12

$$s^{L}_{g} \sum_{j \in J} GP^{L}_{j,p,t} = NP_{p,t} \quad \forall p \in P, t > 1 \tag{12}$$

Plants, Pipelines, and Compressors Sizing. Separation Plants. The total processing capacity of a plant p at time t ($SepCap_{p,t}$) is given in million m^3 of shale gas per day, and can be calculated from its capacity at the previous period $(t-1)$ plus the capacity expansion started at the beginning of period $(t - \tau s)$, that is, $SepInst_{p,t\ -\ \tau s}$. In other words, it is assumed that separation plants installations/expansions take τs time periods, as stated by Eq. 13

$$SepCap_{p,t} = SepCap_{p,t-1} + SepInst_{p,t-\tau s} \quad \forall p \in P, t > 1 \tag{13}$$

Upper Bound on the Shale Gas Flows Converging to a Separation Plant. The sum of the shale gas flows coming from one or several junction nodes to a single separation plant during every period t should not exceed its processing capacity as expressed by Eq. 14

$$\sum_{j \in J} GP_{j,p,t} \leq SepCap_{p,t} \quad \forall p \in P, t > 1 \tag{14}$$

Installation of Gas Pipelines. As shown in Appendix A, given the gas inlet and outlet pressures, the fluid properties and the pipeline length, maximum gas flows are directly proportional to the pipeline diameter to the power of 2.667. It is also assumed that both raw and dry gases are ideal mixtures of ideal gases. To preserve linearity in the constraints, the diameter of the pipeline installed between a pair of nodes during a certain time period (a model decision) is substituted by a variable that stands for such diameter raised to the power of 2.667. In other words, the model variables $DFP_{i,j,t}$, $DGP_{j,p,t}$, and $DTP_{p,k,t}$ stand for the diameters of the pipelines installed at period t between nodes i-j, j-p, and p-k, respectively, raised to the power of 2.667.

In summary, the gas pipeline flows with regards to pipeline diameters are calculated by Eqs. 15–17

$$FPFlow_{i,j,t} = k_{i,j} l_{i,j}^{-0.5} DFP_{i,j,t} \quad \forall i \in I, j \in J, t > 1 \tag{15}$$

$$GPFlow_{j,p,t} = k_{j,p} l_{j,p}^{-0.5} DGP_{j,p,t} \quad \forall j \in J, p \in P, t > 1 \tag{16}$$

$$TPFlow_{p,k,t} = k_{p,k} l_{p,k}^{-0.5} DTP_{p,k,t} \quad \forall p \in P, k \in K, t > 1 \tag{17}$$

Due to Assumption 9, parameters $k_{i,j}$, $k_{j,p}$, and $k_{p,k}$ take fixed values that can be calculated as shown in Appendix A.

Distances between every pair of nodes ($l_{i,j}$, $l_{j,p}$, and $l_{p,k}$) are also given data.

Maximum Gas Flow between a Pair of Nodes. The maximum gas flow between every pair of nodes depends on the size of the pipelines installed in previous periods, plus the additional flow capacity added due to a recent pipeline construction, as stated by Eqs. 18–20. It is assumed that pipelines are installed from period $(t-\tau p)$ to $(t-1)$ and are not able to transport gas until the period t, τp being the pipeline construction lead time, in quarters

$$\mathrm{FPCap}_{i,j,t}=\mathrm{FPCap}_{i,j,t-1}+\mathrm{FPFlow}_{i,j,t-\tau p} \quad \forall i \in I, j \in J, t>1 \tag{18}$$

$$\mathrm{GPCap}_{j,p,t}=\mathrm{GPCap}_{j,p,t-1}+\mathrm{GPFlow}_{j,p,t-\tau p} \quad \forall j \in J, p \in P, t>1 \tag{19}$$

$$\mathrm{TPCap}_{p,k,t}=\mathrm{TPCap}_{p,k,t-1}+\mathrm{TPFlow}_{p,k,t-\tau p} \quad \forall p \in P, k \in K, t>1 \tag{20}$$

Finally, shale gas and dry gas flows at every time period are bounded by the flow capacity connecting every pair of nodes, as enforced by Eqs. 21–23

$$\mathrm{FP}_{i,j,t} \le \mathrm{FPCap}_{i,j,t} \quad \forall i \in I, j \in J, t>1 \tag{21}$$

$$\mathrm{GP}_{j,p,t} \le \mathrm{GPCap}_{j,p,t} \quad \forall j \in J, p \in P, t>1 \tag{22}$$

$$\mathrm{TP}_{p,k,t} \le \mathrm{TPCap}_{p,k,t} \quad \forall p \in P, k \in K, t>1 \tag{23}$$

Installation of Liquid Pipelines. By Assumption 10, a maximum mean velocity is imposed to liquid flows to make sure that head losses remain at specified values. In liquid pipeline network design, a typical value used is $v^{\max}=1.5$ m/s. Under such an assumption, liquid flows are directly proportional to the pipeline section, and by extension, directly proportional to the pipeline diameter raised to the power of 2. As for gas pipelines, the diameter of a liquid pipeline installed between a gas processing plant p and a petrochemical plant l during a certain time period (a model decision) is substituted by an analogous variable, which stands for such diameter to the power of 2 (variable $\mathrm{DLP}_{p,l,t}$). As a result, liquid pipeline flows (given in tons per day) with regards to pipeline diameters are calculated by Eq. 24

$$\mathrm{LPFlow}_{p,l,t}=k_{p,l}\mathrm{DLP}_{p,l,t} \quad \forall p \in P, l \in L, t>1 \tag{24}$$

where $k_{p,l}=3600 \times 24 \times \rho \ \pi \ {v_{p,l}}^{\max}/4$, ρ is the liquid (ethane) density given in ton/m^3, and ${v_{p,l}}^{\max}$ the maximum mean velocity, in m/s.

Maximum Flow in Liquid Pipelines. Similarly to gas pipelines, the model decides when to install a new pipeline and of what size. Equation 25 determines the flow capacity of every liquid pipeline at every time period (in ton/day), whereas constraint 26 imposes such value as an upper bound on the liquid flow from p to l during period t

$$\mathrm{LPCap}_{p,l,t}=\mathrm{LPCap}_{p,l,t-1}+\mathrm{LPFlow}_{p,l,t-\tau p} \quad \forall p \in P, l \in L, t>1 \tag{25}$$

$$\mathrm{LP}_{p,l,t} \le \mathrm{LPCap}_{p,l,t} \quad \forall p \in P, l \in L, t>1 \tag{26}$$

Power of Compressors. If the suction and discharge pressures are given (see Assumption 9), and assuming that compressors are adiabatic, a simple expression can be derived to calculate the required compression power (in kW) as shown in Appendix A. Under such assumptions, the required power is directly proportional to the total flow of gas being compressed. In the case of raw gas, compressed at junction nodes and sent to processing plants, the total power installed up to time t ($\mathrm{JCP}_{j,t}$) must be equal or greater than the power demanded by the total flows of raw gas compressed by j at time t, as expressed by Eq. 27

$$\mathrm{JCP}_{j,t} \ge kc_j \sum_{p \in P} \mathrm{GP}_{j,p,t} \quad \forall j \in J, t>1 \tag{27}$$

Similarly, the power of compressors installed at the outlet of the processing plant p up to time t ($\mathrm{PCP}_{p,t}$) sending dry gas to demand nodes k (typically, gas distribution companies) is lower-bounded by constraint 28

$$\mathrm{PCP}_{p,t} \ge kc_p \sum_{k \in K} \mathrm{TP}_{p,k,t} \quad \forall p \in P, t>1 \tag{28}$$

Moreover, compressor stations can be expanded in the planning horizon by installing new compressors at the same node. Equations 29 and 30 determine the total power of compressors installed up to time t at nodes j and p, respectively. τc is the compressor installation lead time in quarters

$$\mathrm{JCP}_{j,t}=\mathrm{JCP}_{j,t-1}+\mathrm{JCInst}_{j,t-\tau c} \quad \forall j \in J, t>1 \tag{29}$$

$$\mathrm{PCP}_{p,t}=\mathrm{PCP}_{p,t-1}+\mathrm{PCInst}_{p,t-\tau c} \quad \forall p \in P, t>1 \tag{30}$$

Water Supplies. Water Demand for Drilling and Fracturing Wells. As explained before, a large amount of freshwater is required in the shale gas industry for the hydraulic fracturing of new wells. This model assumes that the total amount of water required by a single well during the drilling, fracturing, and completion processes (wr_i) is known (typically, 20,000 m^3/well) but may depend on the well location. Equation 31 states that the total number of wells drilled, fractured, and completed in pad i during period t determines the total water requirement of that pad at that period, and such amount should be supplied from one or more freshwater sources f. The amount of freshwater supplied by source f for drilling and fracturing new wells in pad i during period t is a key model decision represented by the continuous variable $\mathrm{WS}_{f,i,t}$. In addition, if the well-pad i has the infrastructure for flowback water treatment and reuse, a reuse factor rf_i (usually below 20%) can reduce the need for freshwater, as shown in the LHS of Eq. 31

$$N_{i,t}\mathrm{wr}_i/(1+\mathrm{rf}_i) = \sum_{f \in F} \mathrm{WS}_{f,i,t} \quad \forall i \in I, t \in T \tag{31}$$

Water Availability. Every freshwater resource (nearby rivers, lakes, underground water and so forth) usually has an upper limit on the amount of water that can provide to the shale gas industry often given by a seasonal profile. If the parameter $\mathrm{fwa}_{f,t}$ stands for the maximum volume of freshwater that source f can supply to the drilling and fracturing of new wells during the whole period t, the total amount supplied from f to every pad i should be upper-bounded as in constraint 32

$$\sum_{i \in I} \mathrm{WS}_{f,i,t} \le \mathrm{fwa}_{f,t} \quad \forall f \in F, t \in T \tag{32}$$

Maximum Demands. A critical model decision is where to sell both the dry gas and the ethane flows produced by the shale gas processing plants. Every potential market (or demand node) is assumed to consume a maximum amount of product (dry gas for gas distributors and ethane for petrochemical plants) based on their own transportation or processing capacities. Moreover, such demand profile can be

seasonal, especially in dry gas markets. Constraints 33 and 34 finally restrict the total flow of dry gas and ethane that can be sent from processing plants to each demand node during every period of the planning horizon

$$\sum_{p\in P} \mathrm{TP}_{p,k,t} \le \mathrm{gasdem}_{k,t} \quad \forall k \in K, t > 1 \tag{33}$$

$$\sum_{p\in P} \mathrm{LP}_{p,l,t} \le \mathrm{ethdem}_{l,t} \quad \forall l \in L, t > 1 \tag{34}$$

Objective function

The model objective is to maximize the NPV of the long-term planning project, as expressed in Eq. 35

$$\begin{aligned}
\mathrm{NPV} = &\sum_{t\in T} (1+\mathrm{dr}/4)^{-t} \\
&\Bigg[\sum_{p\in P}\sum_{k\in K} \mathrm{gasp}_{k,t} nd_t \mathrm{TP}_{p,k,t} + \sum_{p\in P}\sum_{l\in L} \mathrm{ethp}_{l,t} nd_t \mathrm{LP}_{p,l,t} + \sum_{p\in P} \mathrm{lpgp}_t nd_t \mathrm{NP}_{p,t} \\
&- \sum_{i\in I}\sum_{j\in J} \mathrm{shgc}_{i,t} nd_t \mathrm{FP}_{i,j,t} \\
&- \sum_{i\in I}\sum_{n=1}^{\bar{n}_i} kd\ n^{\mathrm{WellExp}} y_{i,n,t} \\
&- \sum_{p\in P} ks\ \mathrm{SepInst}_{p,t}{}^{\mathrm{SepExp}} \\
&- \sum_{i\in I}\sum_{j\in J} kp\ l_{i,j} \mathrm{DFP}_{i,j,t}{}^{\mathrm{GasPipeExp}} - \sum_{j\in J}\sum_{p\in P} kp\, l_{j,p} \mathrm{DGP}_{j,p,t}{}^{\mathrm{GasPipeExp}} \\
&- \sum_{p\in P}\sum_{k\in K} kp\ l_{p,k} \mathrm{DTP}_{p,k,t}{}^{\mathrm{GasPipeExp}} - \sum_{p\in P}\sum_{l\in L} kp\, l_{p,l} \mathrm{DLP}_{p,l,t}{}^{\mathrm{LiqPipeExp}} \\
&- \sum_{j\in J} kc \mathrm{JCInst}_{j,t}{}^{\mathrm{CompExp}} - \sum_{p\in P} kc \mathrm{PCInst}_{p,t}{}^{\mathrm{CompExp}} \\
&- \sum_{f\in F}\sum_{i\in I} \left(\mathrm{fix}_f + \mathrm{var}_f l_{f,i}\right) \mathrm{WS}_{f,i,t}\Bigg] + (1+\mathrm{dr}/4)^{-T} \sum_{t\in T}\sum_{i\in I} kr_{i,T-t} N_{i,t}
\end{aligned} \tag{35}$$

The objective function comprises positive and negative terms for every period of the planning horizon, discounted back to its present value by the annual discount rate of the project, dr. Positive terms are dry gas sales income, ethane sales income, and NGL other than ethane sales income. Negative terms are shale gas acquisition cost (including production, transportation, and other operative costs), the cost of drilling, hydraulic fracturing, and completing shale gas wells, the cost of installing/expanding shale gas processing capacity at separation plants, the cost of constructing new pipelines either for gathering raw gas or distributing dry gas and ethane, the cost of installing new compressor stations at junction nodes and processing plants, and freshwater acquisition and transportation costs for drilling and fracturing purposes. The last term in the objective function is the residual value of the wells. Parameter $kr_{i,a}$ is the value of a single well of age a in pad i, at the end of the time horizon. It is based on the total amount of gas that a well can still produce beyond the end of the time horizon.

It should be noticed that nonlinear expressions standing for economies of scale functions appear in some of the negative terms of Eq. 35, in all the cases featuring exponents between 0 and 1. Hence the objective function can be classified as nonconvex, with strictly concave separable terms. However, all constraints are linear, as was shown in the previous sections.

Cost estimation

Special attention must be paid to the equipment costing in the objective function (35). Regarding shale gas separation plants and gas compressors, typical values for the exponents SepExp and CompExp vary from 0.60 to 0.77.[24] However, a particular case arises in this model for pipeline construction. By Assumption 13, the cost of pipelines also follows an economy of scale function with regards to the pipeline diameter, with a typical exponent of 0.60. However, it should be noticed that pipeline diameters are not directly considered in the model but through the substituted variables $\mathrm{DFP}_{i,j,t}$, $\mathrm{DGP}_{j,p,t}$, $\mathrm{DTP}_{p,k,t}$ (for gas pipelines), and $\mathrm{DLP}_{p,l,t}$ (for liquid pipelines). In fact, such variables account for the diameters raised to the power of 2.667 in the case of gas pipelines, and power 2 in the case of liquid pipelines. Therefore, if 0.60 is considered as exponent for the economy of scale regarding pipeline construction, the values of the exponents GasPipeExp and LiqPipeExp in the objective function (35) will be $0.60/2.667 = 0.225$ and $0.60/2 = 0.30$, respectively (see Appendix).

Model adaptation to account for shale gas composition variations

Relaxing the assumption of uniform shale gas composition so that the gas wetness is dependent of the well location generally complicates the nature of the constraints. To precisely trace the shale gas flows composition, the critical points in the proposed network superstructure are the junction nodes. If splitting flows to more than one separation plant are required, the model needs to incorporate bilinear equations so that the composition of all the outgoing flows takes a common value given that junctions are mixing-splitting nodes as stated by Eqs. 36–38

$$\mathrm{GComp}_{j,t} \quad \mathrm{GP}_{j,p,t} = \mathrm{GP}^{\mathrm{G}}{}_{j,p,t} \quad \forall j \in J, p \in P, t > 1 \tag{36}$$

$$\mathrm{EComp}_{j,t} \quad \mathrm{GP}_{j,p,t} = \mathrm{GP}^{\mathrm{E}}{}_{j,p,t} \quad \forall j \in J, p \in P, t > 1 \tag{37}$$

$$\mathrm{LComp}_{j,t} \quad \mathrm{GP}_{j,p,t} = \mathrm{GP}^{\mathrm{L}}{}_{j,p,t} \quad \forall j \in J, p \in P, t > 1 \tag{38}$$

Equations 36–38 include the additional variables $\mathrm{GComp}_{j,t}$, $\mathrm{EComp}_{j,t}$, and $\mathrm{LComp}_{j,t}$ (not dependent on the index p), which are the volume compositions of methane, ethane, and LPG (hydrocarbons other than methane and ethane) in the shale gas, forcing all the flows departing from the junction node j (a mixing-splitting node) to have the same composition. Moreover, individual component flow balances are incorporated to the formulation through Eqs. 39–41

$$\sum_{i\in I} \mathrm{FP}^{\mathrm{G}}{}_{i,j,t} = \sum_{p\in P} \mathrm{GP}^{\mathrm{G}}{}_{j,p,t} \quad \forall j \in J, t > 1 \tag{39}$$

$$\sum_{i\in I} \mathrm{FP}^{\mathrm{E}}{}_{i,j,t} = \sum_{p\in P} \mathrm{GP}^{\mathrm{E}}{}_{j,p,t} \quad \forall j \in J, t > 1 \tag{40}$$

$$\sum_{i\in I} \mathrm{FP}^{\mathrm{L}}{}_{i,j,t} = \sum_{p\in P} \mathrm{GP}^{\mathrm{L}}{}_{j,p,t} \quad \forall j \in J, t > 1 \tag{41}$$

It can be easily seen that Eqs. 36–38, which involve bilinear terms, add significant difficulty to the MINLP model, especially because the feasible region cannot then be modeled with linear constraints. However, the next section presents a particular case in which, even incorporating shale gas composition variations, no bilinear terms have to be added.

Shale Gas Flows Converging to a Single Processing Plant. If the model is intended to select only one of the given locations to install a separation plant (as it is expected due to the high cost of this kind of plants), linear expressions hold as no splitting occurs at junction nodes. The model tendency to select only one plant location is demonstrated in Results section with Example 1.

Under this assumption the model modifications necessary to comply with shale gas composition variations are as follows. First, we include a new binary variable w_p, representing whether the location p is selected to install the plant. As a result, the single plant condition leads to constraints 42 and 43

$$\text{SepCap}_{p,t} \leq \text{sepmax}\, w_p \quad \forall p \in P, t > 1 \tag{42}$$

$$\sum_{p \in P} w_p \leq 1 \tag{43}$$

sepmax is an upper bound on the capacity of a single gas processing plant. Note that although the plant location must be unique, it may be installed and expanded in different time periods.

In this way, upper bounds on the individual product flows emerging from every plant are imposed by constraints 44–46, in place of Eqs. 10–12

$$\max_{i \in I} \{\text{gc}_i\} \sum_{j \in J} \text{GP}_{j,p,t} \geq \sum_{k \in K} \text{TP}_{p,k,t} \quad \forall p \in P, t > 1 \tag{44}$$

$$s_{\text{g}}^{\text{E}} \max_{i \in I} \{\text{ec}_i\} \sum_{j \in J} \text{GP}_{j,p,t} \geq \sum_{l \in L} \text{LP}_{p,l,t} \quad \forall p \in P, t > 1 \tag{45}$$

$$s_{\text{g}}^{\text{L}} \max_{i \in I} \{\text{lc}_i\} \sum_{j \in J} \text{GP}_{j,p,t} \geq \text{NP}_{p,t} \quad \forall p \in P, t > 1 \tag{46}$$

gc_i, ec_i, and lc_i are the volume compositions of methane, ethane, and LPG in the shale gas produced at pad i. Note that by Eq. 14, if the plant is not selected (zero capacity) no shale gas flows can be sent to it, and the LHS of the last inequalities is zero. Finally, individual component balances are given by Eqs. 47–49.

$$\sum_{i \in I} \text{gc}_i \text{SP}_{i,t} = \sum_{p \in P} \sum_{k \in K} \text{TP}_{p,k,t} \quad \forall\, t \in T \tag{47}$$

$$s_{\text{g}}^{\text{E}} \sum_{i \in I} \text{ec}_i \text{SP}_{i,t} = \sum_{p \in P} \sum_{l \in L} \text{LP}_{p,l,t} \quad \forall\, t \in T \tag{48}$$

$$s_{\text{g}}^{\text{L}} \sum_{i \in I} \text{lc}_i \text{SP}_{i,t} = \sum_{p \in P} \text{NP}_{p,t} \quad \forall\, t \in T \tag{49}$$

Equation 47 for the methane balance is illustrated through the simple example depicted in Figure 4, comprising two well-pads, one junction node, the processing plant, and the gas demand node. In summary, the modified MINLP model accounting for shale gas composition variations according to the well site, assuming that a unique processing plant location is to be selected, seeks for minimizing Eq. 35, subject to constraints 1–4, 8, 9, 13–34, and 42–49.

Solution Strategies

Solving the MINLP models described in the previous sections is a very challenging task due to three main reasons: (1) the size of the model is large, (2) the objective function involves nonconcave terms accounting for equipment costs (processing plants, pipelines, and compressors), and (3) such nonlinear functions have unbounded derivatives at zero values. The last two features directly follow from the economies of scale, usually adopted to model the equipment cost variation with regards to the equipment size. In principle, the MINLP model can be solved to global optimality with a spatial branch and bound search method with the use of convex envelops for the concave terms in the objective (the secant). However, given the large size of the MINLP, the problem is intractable with such methods like the ones implemented in BARON, LINDOGLOBAL, and COUENNE.[25] Therefore, in this section a tailored strategy is described for solving the large-scale MINLP problem.

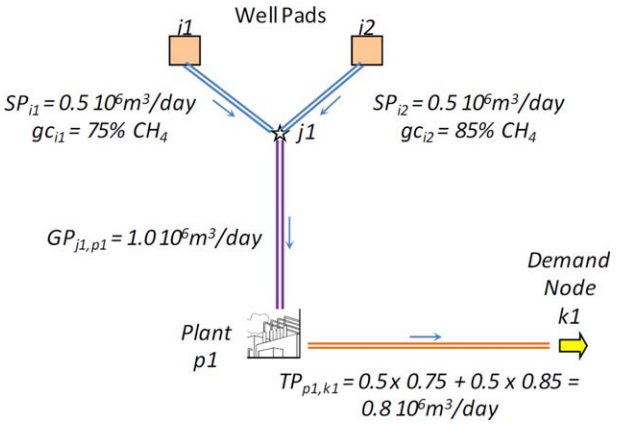

Figure 4. Mixing flows at a single processing plant.

[Color figure can be viewed in the online issue, which is available at wileyonlinelibrary.com.]

Plant and equipment cost estimations

Nonconvex power law expressions of the form $f(x) = c\, x^r$ with exponents less than one as in Biegler et al.,[23] are commonly handled with two approaches: (a) approximate the concave function by a piecewise linear function,[26] and (b) adding a small value ε to the variable x, thus slightly displacing the curve toward the negative values of x. Approximation (a) is computationally costly, but can be useful for generating global upper bounds (GUB) for the maximization problem by solving approximate MILP problems with piecewise linear approximations (underestimations) of the concave equipment cost functions.[27,28] Conversely, approximation (b) is meant to avoid unbounded derivatives but still has drawbacks, especially if the exponents are small.[29] To overcome this problem, a simple expression of logarithmic form is used here. In the following sections, both the piecewise linear approach and the logarithmic approximation used are briefly presented.

Piecewise linear approximation of *concave cost functions*

Given the nonlinear concave cost functions in Eq. 1 [generically referred to as $f(x)$], accounting for the cost $f(x)$ of a processing plant, pipeline, or compressor of size $x \in X$, it is simple to demonstrate that piecewise linear approximations like the one depicted in Figure 5 provide valid underestimations of $f(x)$. That is achieved by partitioning the domain of variable x into intervals ($X = [a_0; a_1] \cup [a_1; a_2] \cup \ldots [a_{m-1}; a_m]$ and introducing binary variables z_v to determine to which interval the selected value of x belongs. At every interval v, function $f(x)$ is approximated by: $\phi(x) = f(x_{v-1}) + (x - x_{v-1})(f(x_v) - f(x_{v-1}))/(x_v - x_{v-1})$. According to Padberg,[30] such a

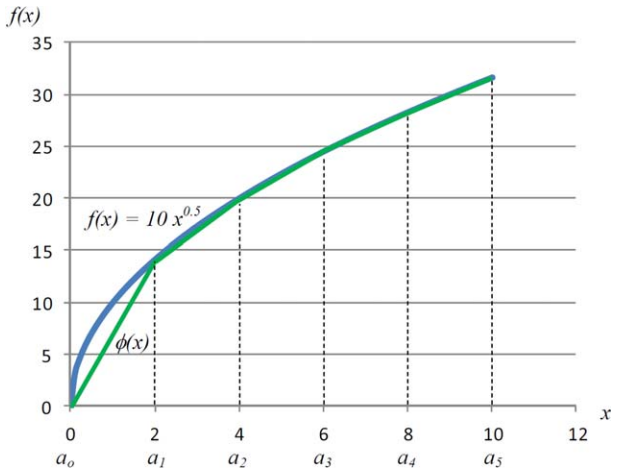

Figure 5. Concave cost function and piecewise linear underestimation.

[Color figure can be viewed in the online issue, which is available at wileyonlinelibrary.com.]

piecewise linearization can be modeled through two formulations: δ and λ. In this case, we adopt the δ-formulation that leads to

$$
\begin{aligned}
x &= a_0 + \sum_{v=1}^{m} y_v \\
\phi(x) &= f(a_0) + \sum_{v=1}^{m} y_v [f(a_v) - f(a_{v-1})]/[a_v - a_{v-1}] \\
y_v &\geq (a_v - a_{v-1}) z_{v+1} \quad \forall v = 1, \ldots, m-1 \\
y_v &\leq (a_v - a_{v-1}) z_v \quad \forall v = 2, \ldots, m \\
y_1 &\leq a_1 - a_0 \\
y_v &\geq 0 \quad \forall v = 1, \ldots, m \\
z_v &\in \{0, 1\} \quad \forall v = 1, \ldots, m
\end{aligned}
\tag{50}
$$

Note that if $z_v = 0$ (with $v > 1$), $y_v = 0$ because of the fourth constraint in formulation 50. From that, z_{v+1} is also zero to satisfy the third constraint, given that $(a_v - a_{v-1})$ is always greater than zero. In other words, $z_v = 0$ implies $z_{v+1} = 0$, or equivalently, $z_{v+1} = 1$ implies $z_v = 1$, for $v > 1$. To illustrate the meaning of the variables in model 50 reconsider the example given in Figure 5. Assume that $x = 6.5$. From the constraints described above, it follows that $z_2 = z_3 = z_4 = 1$, $y_1 = a_1 - a_0 = 2$ (because $z_2 = 1$), $y_2 = a_2 - a_1 = 2$ (because $z_3 = 1$), $y_3 = a_3 - a_2 = 2$ (because $z_4 = 1$), and $y_4 = 0.5$.

By replacing the nonlinear terms in the objective function 35 with the piecewise linear approximations given in model 50, the MINLP model reduces into an MILP model, yielding valid upper bounds for the global optimum of the original problem. A key decision is how to divide the variable domain, that is, how many intervals to consider. The finer the domain discretization, the closer is the upper bound to the actual objective value of the MINLP, but also the higher is the CPU time required by the MILP as the number of integer variables increases significantly. In this case, such a tradeoff is managed through the successive refining strategy presented in a later section, based on the ideas of You and Grossmann,[31,32] dealing with the nonlinear concave function $\sqrt{x}$.

Logarithmic approximation of concave cost functions

To avoid unbounded derivatives and estimation errors when solving non-linear programming (NLP) subproblems in the MINLP model, the alternate approximation function $g(x)$ for $f(x)$ by Cafaro and Grossmann[29] is used

$$
f(x) = cx^r \approx g(x) = k \ln(bx + 1) \tag{51}
$$

where x is the size of the equipment, $f(x)$ is the actual cost of the equipment of size x, $g(x)$ is the estimated cost of the equipment of size x, and k, $b > 0$ are parameters selected to fit $f(x)$ as closely as possible. Further details on this approximation are given in Cafaro and Grossmann.[29]

The proposed function has two main advantages with regards to the classic ε-approximation $f(x) \approx h(x) = c(x + \varepsilon)^r$: (1) the cost of $x = 0$ is exactly zero: $g(0) = k \ln(b\ 0 + 1) = k \ln(1) = 0$, and (2) the derivatives of $g(x)$ for all $x \geq 0$ are bounded positive values given by $g'(x) = b\ k/(b\ x + 1)$. In particular at the origin ($x = 0$), $g'(x) = b\ k$. These properties are particularly useful when dealing with concave cost functions with small exponents, like the cost of pipelines (exponents 0.225 and 0.300, for gas and liquid pipelines, respectively).

Suitable values for parameters k and b in function $g(x)$ can be found relatively easily for liquid and gas pipelines, and the logarithmic approximation leads to very good results (less than 0.50 % error) in the calculation of pipeline costs in all of the case studies tackled in the Results and Discussion section.

Solution algorithm: Branch-Refine-Optimize (BRO) strategy

To find the global optimum of the nonconvex MINLP model presented in the Mathematical Formulation section, a two-level branch-and-refine procedure is proposed (see Figure 6). In the upper level, we successively solve MILP approximations of the original MINLP problem following two purposes: (1) provide valid (and increasingly tighter) upper bounds of the global optimum and (2) propose efficient supply chain network configurations. Once the MILP approximation is solved, the corresponding supply chain network design is fixed by removing all the nodes and arcs of the original superstructure not active in the MILP solution, and the lower level optimizing procedure starts.

The aim of the lower level of the algorithm is to find the global optimal solution of a reduced MINLP problem (or subproblem) only focused on the equipment sizing (plant, pipelines, and compressors) and the drilling strategy (integer variables $n_{i,t}$), as the network structure is fixed. As the reduced MINLP problem is nonconvex, its global optimal solution is found by solving, on the one hand, the reduced MINLP with a nonglobal solver (DICOPT, SBB)[25] to determine a lower bound for the selected network, and then successively partitioning the equipment size domains and recursively solving piecewise linear approximations of the objective function to determine tighter upper bounds (inner loop). Finally, the global optimal solution of the reduced MINLP is a feasible solution of the original MINLP, and its objective value provides a valid global lower bound (GLB) of the problem.

Note that supply chain network designs proposed by the upper level at previous iterations are excluded with integer cuts to reduce the enumeration effort. Such integer cuts are similar to those described by Durán and Grossmann,[8] which eliminate particular binary combinations accounting for

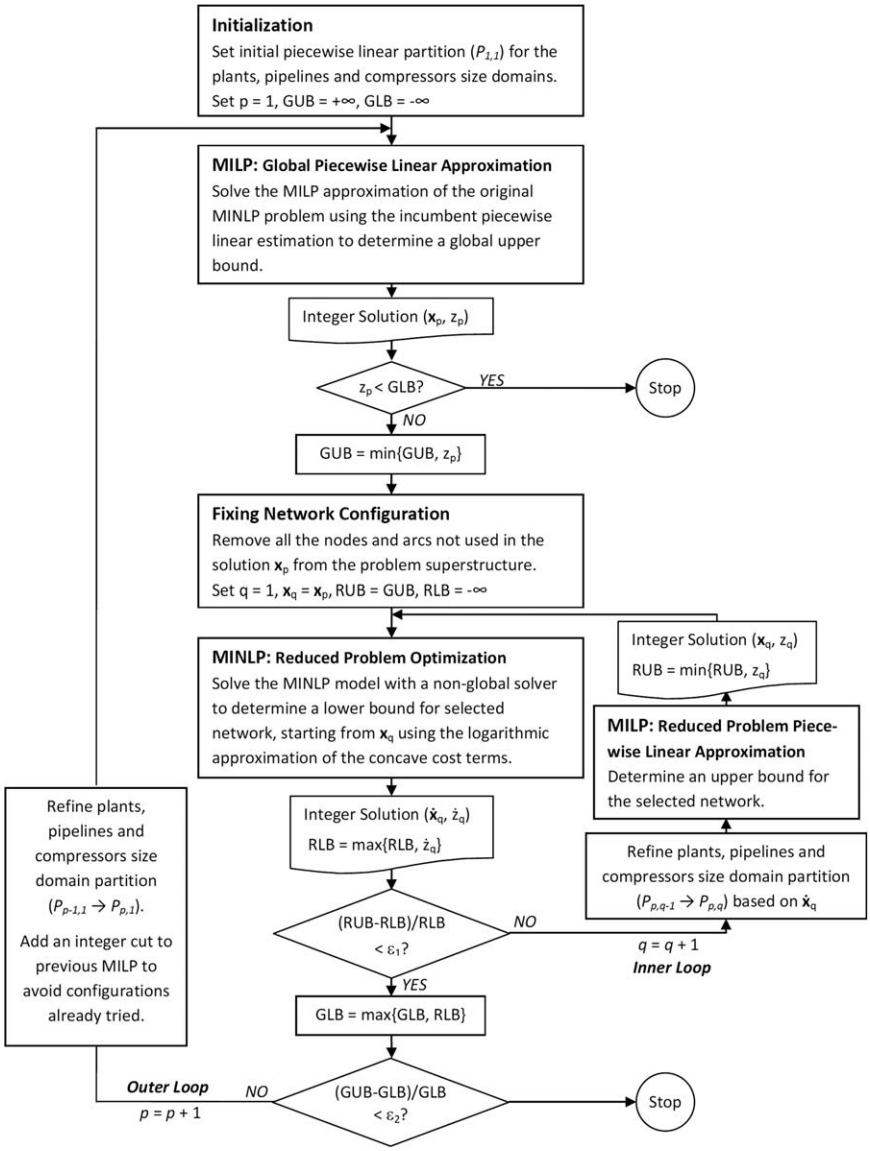

Figure 6. BRO algorithm.

A two-level branch-and-refine procedure for the global optimization of the shale gas supply chain strategic planning.

network configurations already analyzed. The cuts are derived from the values of the binary variables z_v used by the piecewise linear approximation of the concave cost terms in the objective function of the MILP (see Piecewise Linear Approximation of Concave Cost Functions section). As a result, if the approximate solution obtained by the upper level in a new iteration is worse than the best solution found (or GLB), the algorithm automatically stops. Otherwise, the outer loop refines the piecewise linear approximation of the original problem and might improve the network structure so that the global optimal solution can be obtained after a finite number of iterations.

In summary, the proposed solution algorithm is as follows:

Step 1: Initialization. A one-piece linear underestimation (secant) is usually used for all the concave cost terms of later periods (for instance, $t > 10$), whereas in earlier periods the starting piecewise linearization comprises two to four intervals. The GUB is set to $+\infty$, and the GLB $-\infty$.

Step 2. Global Piecewise Linear Approximation. Solving the incumbent MILP approximation of the original MINLP problem (as shown in the Piecewise Linear Approximation of Concave Cost Functions section) provides a GUB. As all the constraints in the MINLP are linear, the optimal solution of the MILP is also a feasible solution of the MINLP problem. Thus, a GLB can be directly obtained by substituting the optimal solution of the MILP into the MINLP. However, this solution can be taken as the initial point of a nonglobal MINLP solving step to improve the GLB.

Step 3. Reduced Problem Optimization. By fixing the network structure, that is, removing all the nodes (well-pads, junctions, gas processing plants, and compressors) and arcs (pipelines) that were not selected in the optimal solution of the MILP, we successively solve a reduced MINLP problem with a nonglobal algorithm (DICOPT or SBB) that is intended to improve the best solution found. The MINLP model makes use of the logarithmic approximation presented in the Logarithmic Approximation of Concave Cost Functions section, which avoids the numerical difficulties reported by You and Grossmann.[31] In this way, solving the nonconvex reduced MINLP might yield an improved lower bound for the subproblem (reduced-problem lower bound or RLB). Next, based on the optimal values of the equipment

size variables, we bisect the corresponding intervals of the piecewise linear approximations. If the optimal solution of the MINLP problem lies at the bounds of some intervals, we do not add a new interval for these terms. After refining the domain partition, we can obtain a tighter upper bound for the reduced problem (reduced-problem upper bound or RUB), as shown in the next step.

Step 4. Reduced Problem Piecewise Linear Approximation. The MILP with the piecewise linear approximation of the reduced problem provides an upper bound RUB, whose value tends to decrease as the domain partition is refined. The inner optimization loop iterates until the lower bound from the MINLP and upper bound of the MILP are within an optimality tolerance ε_1. Once that occurs, the global optimum of the reduced problem has been found, and the lower bound of the original problem (GLB) is updated.

Step 5. Stopping Criteria. From the values of the variables in the best solution found by the reduced MINLP, the intervals of the piecewise linear approximations in the original problem are bisected, and a new integer cut is added to the upper level MILP to avoid network configurations already tried. Next, the algorithm returns to Step 2 and two cases may occur: (a) a tighter GUB is found or (b) the approximate solution is worse than the GLB. In case (a), the main optimization loop keeps iterating until the global lower and upper bounds are close enough to satisfy the optimality criteria ε_2 ($> \varepsilon_1$). In case (b), the algorithm stops and the optimal solution is the best solution found.

Results and Discussion

To illustrate the application of the MINLP model and the proposed optimization algorithm, three examples are considered in this section. Example 1 deals with a real-size illustrative problem for optimizing the supply chain network design for a new shale gas exploitation area covering more than 10,000 km^2. In this case, a different production profile is assumed for each potential site where the wells are drilled. However, the gas "wetness" (or hydrocarbon composition) is assumed to be the same in each well-pad. Example 2 is a variant of the previous case where the gas wetness becomes dependent on the well location. The aim of the second example is twofold: (a) find out how the gas wetness distribution affects the drilling strategy and (b) highlight the contribution of the hydrocarbons other than methane to the economics of the project. The third example introduces variations in the pipeline pressures in order to show changes in the optimal solution. Finally, a real-world case study of the U.S. shale gas industry is tackled at the end of this section.

Example 1: The same shale gas wetness in all the wells

Consider the shale gas supply chain superstructure whose nodes are shown in Figure 7. It comprises nine potential sites for drilling wells ($i1 \ldots i9$), eight potential sites for junction/compression nodes ($j1 \ldots j8$), three possible sites for processing plant installation ($p1 \ldots p3$), three methane demanding nodes ($k1 \ldots k3$), three ethane demanding nodes ($l1 \ldots l3$), and three freshwater sources ($f1 \ldots f3$). The Cartesian coordinates of each site (in km) are given in Table 1. Distances between nodes for pipeline length and water transportation calculations are measured in Euclidean norm.

The planning horizon comprises 40 time periods (quarters) and the annual rate that was considered for discounting back cash flows is 13.5%. The methane price is assumed to be seasonal, with a base price of \$0.14286/m^3 for periods $t1$, $t5$, $t9$, ..., and seasonality factors of 1.10 for periods $t2$, $t6$, $t10$, ...; 1.25 for $t3$, $t7$, $t11$, ...; and 1.10 for $t4$, $t8$, $t12$, ... The shale gas unit production cost is fixed at \$396.82/10^{6}m^3, the price of liquid ethane is \$329.48/ton, and other hydrocarbons (heavier than ethane) are LPGs (propane, butanes, and pentanes) separately sold at \$749.56/ton (more than double of the ethane price). The liquid ethane density is 0.546 ton/m^3, whereas the LPG density is averaged at 0.600 ton/m^3. Maximum methane demands are 10, 5, and 15 $\times$ 10^6 m^3/day for nodes $k1$, $k2$, and $k3$, whereas maximum ethane demands at nodes $l1$, $l2$, and $l3$ are 2500, 2000, and 1500 ton/day, respectively. LPG maximum demands are 3000 ton/day at every node p.

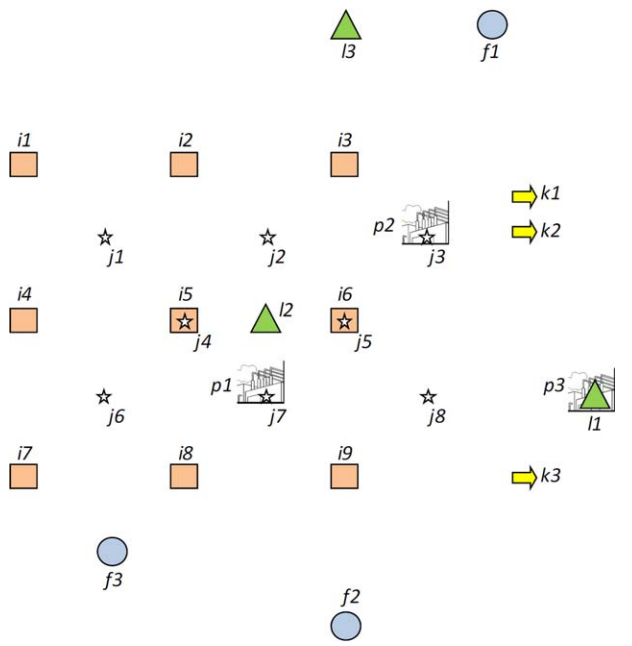

Figure 7. Nodes of the supply chain network superstructure for Examples 1, 2, and 3.

[Color figure can be viewed in the online issue, which is available at wileyonlinelibrary.com.]

Freshwater availability is also assumed to be seasonal with reference values of 250, 80, and 190 $\times$ 10^3 m^3/quarter for sources $f1$, $f2$, and $f3$, respectively, and seasonality factors of 1.20 for periods $t1$, $t5$, $t9$, ...; 1.00 for periods $t2$, $t6$, $t10$, ...; 0.80 for $t3$, $t7$, $t11$, ...; and 1.10 for $t4$, $t8$, $t12$, ... Every individual well requires 20,000 m^3 to be drilled and hydraulically fractured, regardless of its location. Moreover, no more than three wells can be drilled in a single location during one quarter, and a total of 20 wells is the maximum number permitted for a single well-pad. Overall, a total of 180 wells can be drilled over the time horizon.

The shale gas pressure at well-pads is set to 2.1 MPa, compressors at junction nodes increase the shale gas pressure from 1.4 to 2.1 MPa, processing plants receive the shale gas at 1.4 MPa, whereas compressors increase the methane pressure from 4.0 to 6.0 MPa. Finally, methane is delivered at demand nodes at 4.0 MPa.

Regarding the cost of processing plants, wells, and compressors (in million U.S. dollars or USD), economies of scale functions of the form $C(x) = c\ x^r$ are used, with $c = 210$, 5, 0.011150, and $r = 0.60$, 0.60, 0.77, respectively. The units of the size variables are 10^6 m^3/day for plants, wells for drilling/fracturing, and kW for compressors. For costing

Table 1. Cartesian Coordinates of Problem Nodes (in km)

	Well Pads									Junction Nodes								Processing Plants			Methane Demand Nodes			Ethane Demand Nodes			Freshwater Sources		
	*i*1	*i*2	*i*3	*i*4	*i*5	*i*6	*i*7	*i*8	*i*9	*j*1	*j*2	*j*3	*j*4	*j*5	*j*6	*j*7	*j*8	*p*1	*p*2	*p*3	*k*1	*k*2	*k*3	*l*1	*l*2	*l*3	*f*1	*f*2	*f*3
x	0	50	100	0	50	100	0	50	100	25	75	125	50	100	25	75	125	75	125	175	145	145	145	175	75	100	150	100	25
y	0	0	0	50	50	50	100	100	100	25	25	25	50	50	75	75	75	75	25	75	15	25	100	75	50	−50	−50	150	125

pipelines, a function $C(l,D) = c\ \ l\ \ D^r$ is used, with $c = 0.125594$, $r = 0.60$, l (length) measured in km, and D (diameter) in inches. The same function is used regardless of the product transported (liquid or gas) and the nodes being joined. For instance, the cost of a pipeline of 10 inches in diameter and 100 km in length is 50 million USD.

From experimental data, the shale gas productivity (10^6 m^3/day) at every well is approximated by a discrete-time decreasing function of the well age t with the form $P(t) = k_i\ t^{-0.37}$, for $t = 1, \ldots, 40$. The constant k_i is 0.0806 for wells drilled in locations $i = i1$, $i4$; 0.0732 for $i = i2$, $i5$, $i7$; 0.0659 for $i = i3$, $i6$, $i8$; and 0.0586 for $i = i9$. Finally, the shale gas composition (independent of the well location) and its water content are given in the second column of Table 2. Notice the relatively high composition of wet gas (about 25%, with half of it being ethane).

After implementing the BRO solution algorithm for this example, we find the optimal design for the shale gas supply chain depicted in Figure 8, and a strategic drilling plan yielding an NPV of 1664.48 million USD. The optimal solution determines that only one shale gas processing plant is installed at site $p1$, with a maximum capacity of 6.594×10^6 m^3 of shale gas per day and a total cost of 651.2 million USD. Due to the economies of scale, the plant and all the pipelines are installed in the first period of the time horizon, with no expansions planned over the first 10 years. Regarding shale gas compression power at junction nodes, 1236, 706, and 818 kW are installed at nodes $j4$, $j5$, and $j6$, in that order.

The selected destinations for methane and ethane are nodes $k3$ and $l2$, respectively. Methane is supplied by a gas pipeline of 74.33 km in length and 17 $^1/_2$ inches in diameter (or the upper closest diameter for gas commercial pipelines), requiring a compressor of 2428 kW. In turn, ethane is transported through a liquid pipeline of 5 $^3/_4$ inches in diameter. The maximum flow for both pipelines is reached in quarter $t7$, when the plant is operated at full capacity to produce methane at the rate of 4.915×10^6 m^3/day, and ethane at 1130 ton/day (see Figure 9). The production level at the plant remains high for another six quarters until the maximum number of wells at every pad (20) is reached.

One of the important features of the model is the ability to generate an optimal drilling strategy so as to keep the level of production well balanced over the entire time horizon (see Figure 9). In this way, plant, compressor, and pipeline sizes can be smaller than those needed when a very intensive drilling plan is applied.

The optimal drilling plan is depicted in Figure 10. The height of each single-colored column at every line (which can be 0, 1, 2, or 3) represents the number of wells being drilled at each location in every period. The drilling plan is developed over the first 3 years of the planning horizon, and two phases can be easily distinguished: (1) Intensive drilling phase and (2) flow maintenance phase. The first phase covers the first five quarters, and its main objective is to drill and fracture as many wells as possible as there are no wells at the initial time. However, this strategy is partially limited by the water availability, which is scarce in periods $t2$ and $t3$. Even under these circumstances, the model tends to rapidly increase the shale gas production focusing on the most productive regions. The second drilling phase takes place during the following six quarters, and seeks to maintain a stable flow of shale gas in every pipeline, until the maximum number of wells (20) is reached in every well-pad.

Table 2. Shale Gas Water Content (kg/10^6 m^3) and Composition (mol % in Dry Basis)

		Example 2								
	Example 1	*i*1	*i*2	*i*3	*i*4	*i*5	*i*6	*i*7	*i*8	*i*9
H_2O (kg/10^6 m^3)	615	615	615	615	615	615	615	615	615	615
N_2 (mol %)	1.0	1.0	1.0	1.0	1.0	1.0	1.0	1.0	1.0	1.0
CO_2 (mol %)	1.0	1.0	1.0	1.0	1.0	1.0	1.0	1.0	1.0	1.0
CH_4 (mol %)	74.6	87.6	83.6	80.6	82.6	80.6	77.6	78.6	75.6	74.6
C_2H_6 (mol %)	12.8	5.8	7.8	8.8	9.8	9.8	11.8	10.8	12.8	12.8
C_3H_8 (mol %)	7.6	3.6	4.6	5.6	4.6	5.6	5.6	6.6	6.6	7.6
i-C_4H_{10} (mol %)	1.2	0.5	0.7	1.2	0.5	0.8	1.1	0.7	0.8	1.2
n-C_4H_{10} (mol %)	0.8	0.2	0.3	0.8	0.2	0.2	0.9	0.3	0.7	0.8
i-C_5H_{12} (mol %)	0.5	0.2	0.5	0.5	0.2	0.7	0.5	0.7	1.0	0.5
n-C_5H_{12} (mol %)	0.5	0.1	0.5	0.5	0.1	0.3	0.5	0.3	0.5	0.5

Overall, the optimal strategy yields a positive NPV of 1664.48 million USD, with a total investment in period *t*1 amounting to 1077.60 million USD. Of the initial investment, 60% corresponds to the gas processing plant, 30% to pipeline installation, 8% to well drilling and fracturing costs, 1% to compressors, and less than 1% to water acquisition and transportation charges. Finally, the discounted payback period of the project is 3 years. Most of the project revenues come from LPG sales (50%) followed by methane (34%) and at last ethane (16%). It is interesting to note that if we install two processing plants (*p*1 and *p*2) instead of only one, the resulting NPV reduces to only one-third of the optimal NPV. The next example is proposed to analyze how the solution changes when the shale gas wetness depends on the well location, with the gas being much drier in some regions.

Example 2: Variable shale gas wetness

The second example is a variant of Example 1 in which the shale gas wetness is dependent on the well site. The shale gas composition with regard to the location is presented in Table 2 where it can be seen that the composition of wet gas is less than 25% in many well-pads. The only site producing shale gas with exactly the same composition as in Example 1 is node *i*9. The shale gas becomes drier in the direction of node *i*1. In fact, the methane mole percentage increases from 74.6% (node *i*9) to 87.6% (node *i*1). All the other data remain unchanged. Regarding the MINLP model, we use the modified version of the model presented in the Shale Gas Flows Converging to a Single Processing Plant section, which preserves linearity in the constraints under the assumption that a unique processing plant is installed. Comparing the solution with the one obtained in Example 1, it can be concluded that the assumption of a single processing plant installation is not such a restrictive assumption for our case study.

In fact, the optimal network configuration obtained is exactly the same as for Example 1. This is an expected result as the total amount of shale gas produced in every pad is the same. There are only minor variations in the pipeline diameters, compressor power, and processing plant size. In particular, the plant capacity is reduced from 6.594 to 6.222 $\times$ 10^6 m^3/day due to a more extended drilling strategy. The main differences in the shale gas composition definitively affect the drilling strategy, as well as the economics of the project. As shown in Figure 11, the optimal drilling strategy now tends to prioritize the pads producing wetter gas (i.e., those producing a higher amount of heavier hydrocarbons). Wells drilled in less attractive pads (*i*1, *i*2, *i*3, *i*4, *i*5) are left for later periods (*t*8–*t*13). As a result, the overall drilling strategy now takes 13 periods instead of 11.

From Figure 12, it can be seen that the production of methane is extended through a longer period of time, but the amount of ethane and heavier hydrocarbons is significantly lower than in Example 1. In summary, the optimal strategic plan involves an initial investment of 1054.67 million USD, whereas the NPV is 1202.54 million USD, 27.8% below the NPV for Example 1. As a consequence, the discounted

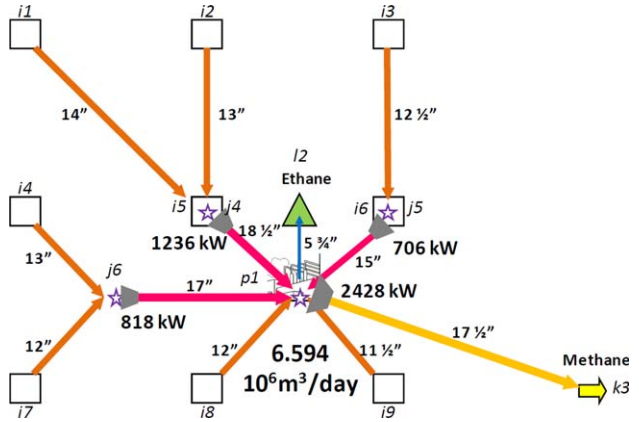

Figure 8. Optimal design for the shale gas supply chain network of Example 1.

[Color figure can be viewed in the online issue, which is available at wileyonlinelibrary.com.]

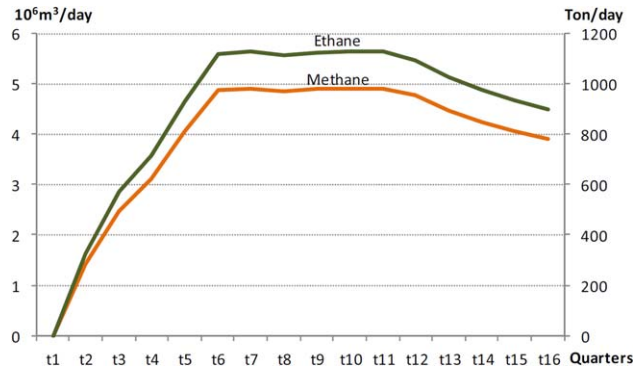

Figure 9. Amount of methane and ethane produced during the first 4 years in the optimal solution of Example 1.

[Color figure can be viewed in the online issue, which is available at wileyonlinelibrary.com.]

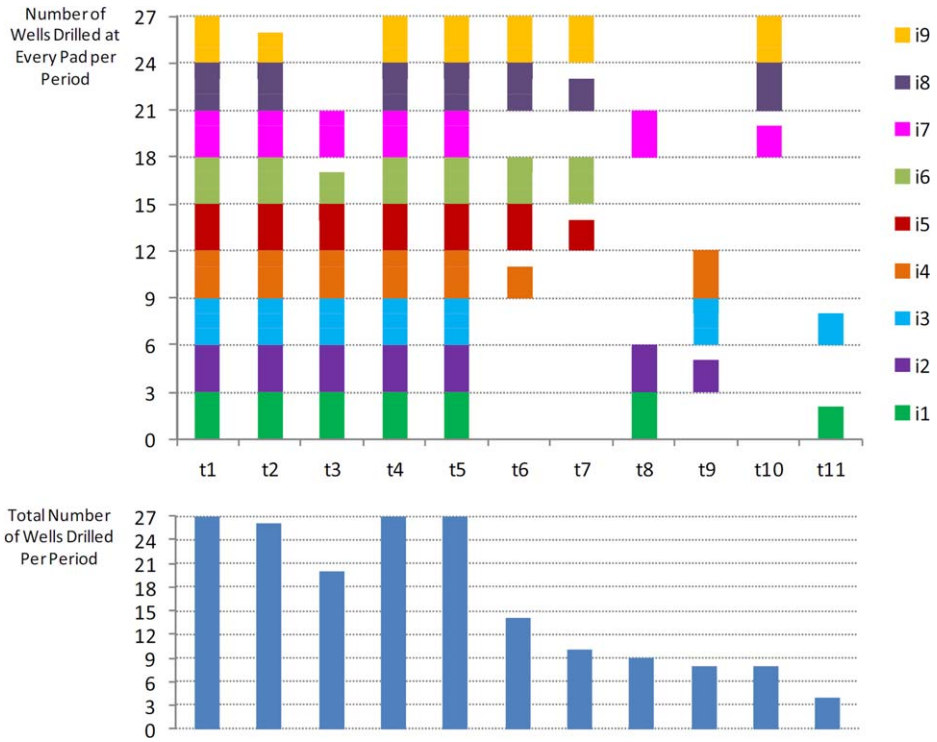

Figure 10. Optimal drilling strategy for Example 1.

[Color figure can be viewed in the online issue, which is available at wileyonlinelibrary.com.]

payback period increases from 3 to 3.7 years. The economic differences can be clearly noticed in the product sales income distribution. Given the new shale gas composition for each well-pad, LPG and methane sales each represent 43% of the total income, whereas ethane is only 14%; vs. 50%, 34% and 16% in the previous example.

Example 3: Changes in gas pipeline pressures

By Assumption 9, all the gas pressures are specified at some fixed values before solving the model. In Examples 1 and 2, the shale gas pipeline pressures vary from 2.1 MPa (inlet pressure) to 1.4 MPa (outlet pressure), whereas transmission pipelines transport dry gas from 6.0 to 4.0 MPa. In

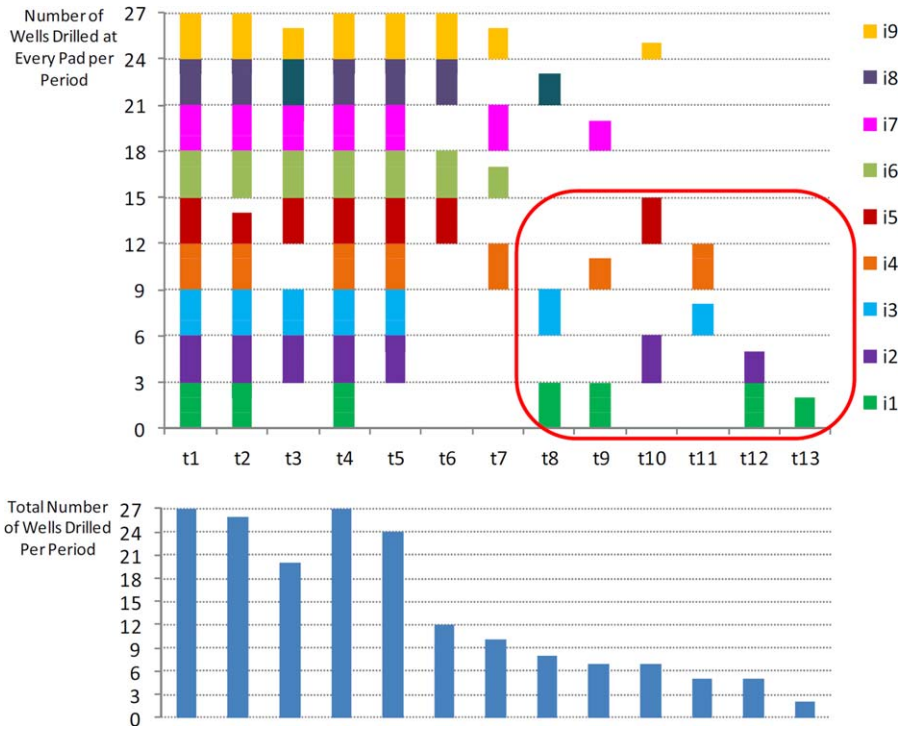

Figure 11. Optimal drilling strategy for Example 2.

[Color figure can be viewed in the online issue, which is available at wileyonlinelibrary.com.]

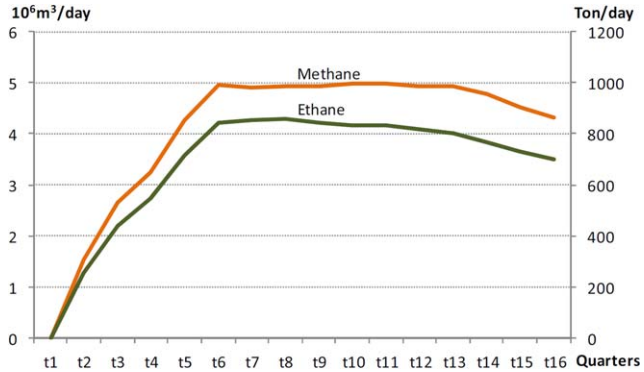

Figure 12. Amount of methane and ethane produced during the first 4 years in the optimal solution of Example 2.

[Color figure can be viewed in the online issue, which is available at wileyonlinelibrary.com.]

both cases, gas compressors are assumed to operate at a common compression ratio of 1.5 (a typical value for centrifugal compressors). Even though determining the optimal pressure for every pipeline is out of the scope for this model, Example 3 is intended to show how the results are affected by changes in the pressure values. Example 3 is a variation of Example 1 in which both shale gas and dry gas compressors operate at a pressure ratio of 2, whereas shale gas at wellbores is delivered at a pressure of 2.8 MPa instead of 2.1 MPa. More precisely, gathering pipelines transport shale gas from 2.8 to 1.4 MPa, whereas dry gas is transported through transmission pipelines from 8.0 to 4.0 MPa.

The main findings of this example are related to pipeline and compressor sizing, as the pipeline network structure, the processing plant size, and the drilling strategy do not change in the optimal solution. As expected, pipeline diameters can be reduced at the expense of using more power in the compressors. On the one hand, the pipeline diameters are reduced by 15.75% (from 12.38 to 10.43 in. on average), the gathering pipelines are reduced by 15.91% (from 16.59 to 13.95 in.) and the gas transmission pipeline by 14.71% (from 17.33 to 14.78 in.). Conversely, shale gas compressors (a total of three, at junction nodes *j*4, *j*5, and *j*6) increase their total power by a factor of 1.71 (from 2760.47 to 4723.31 kW), whereas the only dry gas compressor at the outlet of the processing plant has a total power of 4189.29 kW (3000 kW installed in period *t*1 and the remaining 1189.29 kW in period *t*4), which implies a 72.6% increase in the methane compressor power compared to Example 1.

Overall, the pipeline installation cost is reduced from 321.35 to 291.10 million USD, the investment in compressor stations increases from 11.14 to 17.56 million USD, while the NPV of the project is improved by 1.15%. Although the difference is rather small, future work will focus on determining the optimal pressures for the gas pipelines.

Computational results

The most time-consuming step in the BRO algorithm is the solution of the MILP approximation of the full-size problem, that is, the global piecewise linear approximation. We initialize the algorithm with a one-piece linear underestimation for all the concave cost terms for periods $t > 10$, whereas the starting piecewise linearization involves two to four intervals for $t \leq 10$ (two for pipelines and compressors, four for processing plants). Even under those conditions, the size of the first MILP approximation of Example 1 is rather large: 51,880 equations, 47,643 continuous variables, and 3490 binary variables (2343 after preprocessing) as can be seen in Table 3. From the latter, 1440 determine the number of wells to drill at every period, whereas the remaining are the binaries of the δ piecewise linearization. Even though the relaxation is somewhat tight (16.8% integrality gap), the first MILP takes almost 5 h of CPU time (using GAMS/GUROBI 5.5.0[25] on an Intel Core i7 CPU, 2.93 GHz, 12 GB RAM, with six parallel threads) to solve the problem with an optimality gap of 0.25%. Having solved this problem, the first GUB is found: 1709.04 million USD. Next, the solution found is used as the initial point of a nonglobal MINLP optimization algorithm (GAMS/DICOPT 24.1.3, with GUROBI 5.5.0 as the MILP solver, and CONOPT 3.15 as the NLP solver),[25] which after four major iterations and 190 CPU s finds the first optimized integer solution, yielding an NPV = 1655.83 million USD (3.21% of global optimality gap).

At the next step, the BRO algorithm fixes the network configuration, and the inner loop starts to optimize the reduced MINLP problem, by successively refining piecewise linear approximations of the concave cost terms in the objective function. As observed in the second line of Table 3, the first reduced MILP problem has one half of the variables and equations of the full-size MILP approximation. In fact, the MILP approximations of the reduced problem have small sizes, never requiring more than 60 s to find the optimal solution (0.25% optimality gap). From Table 3, it follows that the optimality gap of the reduced MINLP problem falls below $\varepsilon_1 = 0.10$ after four iterations. At that moment, the algorithm adds an integer cut removing the network

Table 3. Computational Results for Example 1

		MILP				MINLP						
Outer Loop #	Inner Loop #	Cont. Var.	Bin. Var.	Eq.	CPUs	Cont. Var.	Bin. Var.	Eq.	Major Iters.	CPUs	Red Opt. Gap % (ε_1)	Global Opt. Gap % (ε_2)
1	1	47,643	3490	51,880	17,530	31,633	1440	28,900	4	190	3.21	3.21
	2[a]	21,344	3737	24,578	14	5087	1440	5532	3	20	2.12	2.94
	3[a]	21,591	3984	25,072	35	5087	1440	5532	3	13	1.34	2.94
	4[a]	21,817	4210	25,524	44	5087	1440	5532	4	21	0.98	2.88
2[b]	1	47,644	3491	51,883	30,922	31,633	1440	28,900	5	364	2.27	2.27
	2[a]	21,344	3737	24,578	20	5087	1440	5532	4	25	1.60	2.27
	3[a]	21,591	3984	25,072	17	5087	1440	5532	3	7	1.14	2.27
	4[a]	21,798	4191	25,486	25	5087	1440	5532	3	7	0.81	2.27

[a]Network configuration is fixed.
[b]Plant cost estimation is refined.

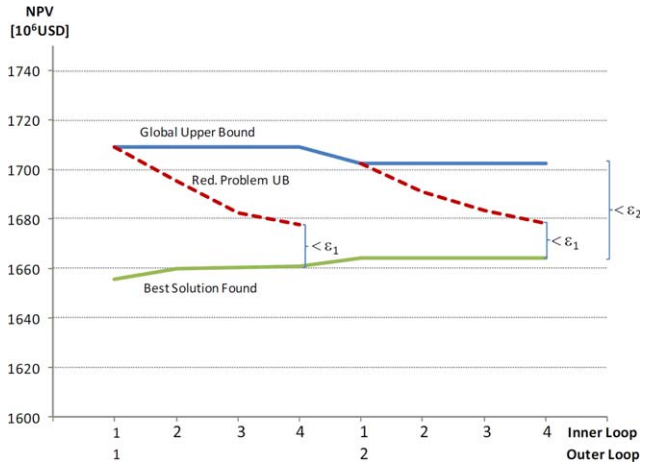

Figure 13. Progress of the GUB, the reduced problem upper bound and the best solution found in the solution of Example 1 through the BRO algorithm.

[Color figure can be viewed in the online issue, which is available at wileyonlinelibrary.com.]

configuration already tried, and refines the full-size MILP piecewise linearization based on the values of the variables at the best solution found.

Even though the size of the MILP does not increase considerably in the second iteration of the outer loop, the time to find the optimal solution increases to 8.5 h. Figure 13 shows the progress of the GUB, the best solution found, and the upper bound for the solution of the reduced problem over two iterations of the outer loop of the BRO algorithm. Overall, after solving eight MILP and eight MINLP models in 13.7 h of CPU time, the global optimality gap is reduced below $\varepsilon_2 = 2.5\%$.

Regarding Example 2, the alternate formulation presented in the Shale Gas Flows Converging to a Single Processing Plant section slightly increases the size of the models compared to Example 1. In the first iteration, the global MILP approximation has 51,998 constraints, 47,643 continuous variables, and 3493 integer variables, taking more than 12 h of computational time to reduce the optimality gap below 1.00%. After two iterations of the outer loop, in more than 24 h of computational time the global optimality gap is 7.5%.

Real-world case study: Shale gas development project

A shale gas production company is interested in expanding the drilling and production activity in the Marcellus shale play. The company has determined more than 150 potential sites for well-pads, which can be grouped into nine regions (see Figure 14). All the shale gas produced in each region is collected by a low-pressure trunk pipeline that transports the gas to a nearby compressor station. Finally, the raw gas is dehydrated and sent through high pressure transmission pipelines tied to midstream lines owned by third party distribution companies. Pipeline construction and compressor installation require considerable lead-times (more than 2 years), which are considered in the formulation. In addition, the company has the possibility of drilling the wells and keeping them closed for some periods until the pipelines collecting the shale gas become available. Such an assumption requires a model adaptation, shown in Appendix B. Besides, a maximum of four wells per pad can be drilled and completed in a single period (up to 12 wells in at most three pads per period) and each pad should not contain more than 10 wells. Fourteen freshwater reservoirs are available in the area. Due to confidentiality reasons, further details on the problem cannot be given.

As the shale gas is dry (95% of methane), the study does not account for gas processing and fractionation plants. However, the large number of pads yields a large-scale MINLP model with 4815 discrete variables, 12,226 continuous variables, and 16,815 constraints. After two major iterations of the BRO algorithm and 71,000 CPUs of computational time, the optimal solution yields an NPV over 815 million USD, with a global optimality gap of 8.2%. The most convenient regions to be exploited during the following 10 years are regions 2 and 6, where a total of 22 and 18 pads are constructed. Gathering pipelines of 7–10 in. in diameter collect the shale gas in each region, while trunk pipelines of 23–24 in., and transmission pipelines of 12 in. (to delivery point 1) and 18 in. (to delivery point 2) are planned. Finally, a compressor station with a total power of 32,000 kW should be installed. Freshwater for drilling and fracturing is supplied by only three of the available reservoirs. Figure 15 shows the drilling strategy used for the 380 selected wells of regions 2 and 6, whereas Figure 16 illustrates the shale gas flows in major pipelines for periods 14–40, showing the tendency of the model for maximizing the pipeline utilization by maintaining a stable flow over time.

Conclusions and Further Work

A new MINLP model for the strategic planning of the shale gas supply chain has been presented in this work. The proposed formulation optimally determines many of the critical decisions to be simultaneously made in the development of a shale gas project: the drilling and fracturing plan over time; the location, sizing, and expansion of gas processing and fractionation plants; the section, length, and location of gas and liquid pipelines (the network configuration); the

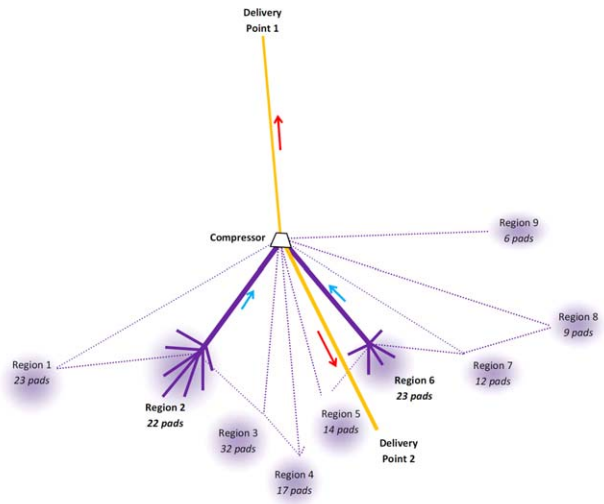

Figure 14. Schematic representation of the shale gas supply chain superstructure for the real-world case.

[Color figure can be viewed in the online issue, which is available at wileyonlinelibrary.com.]

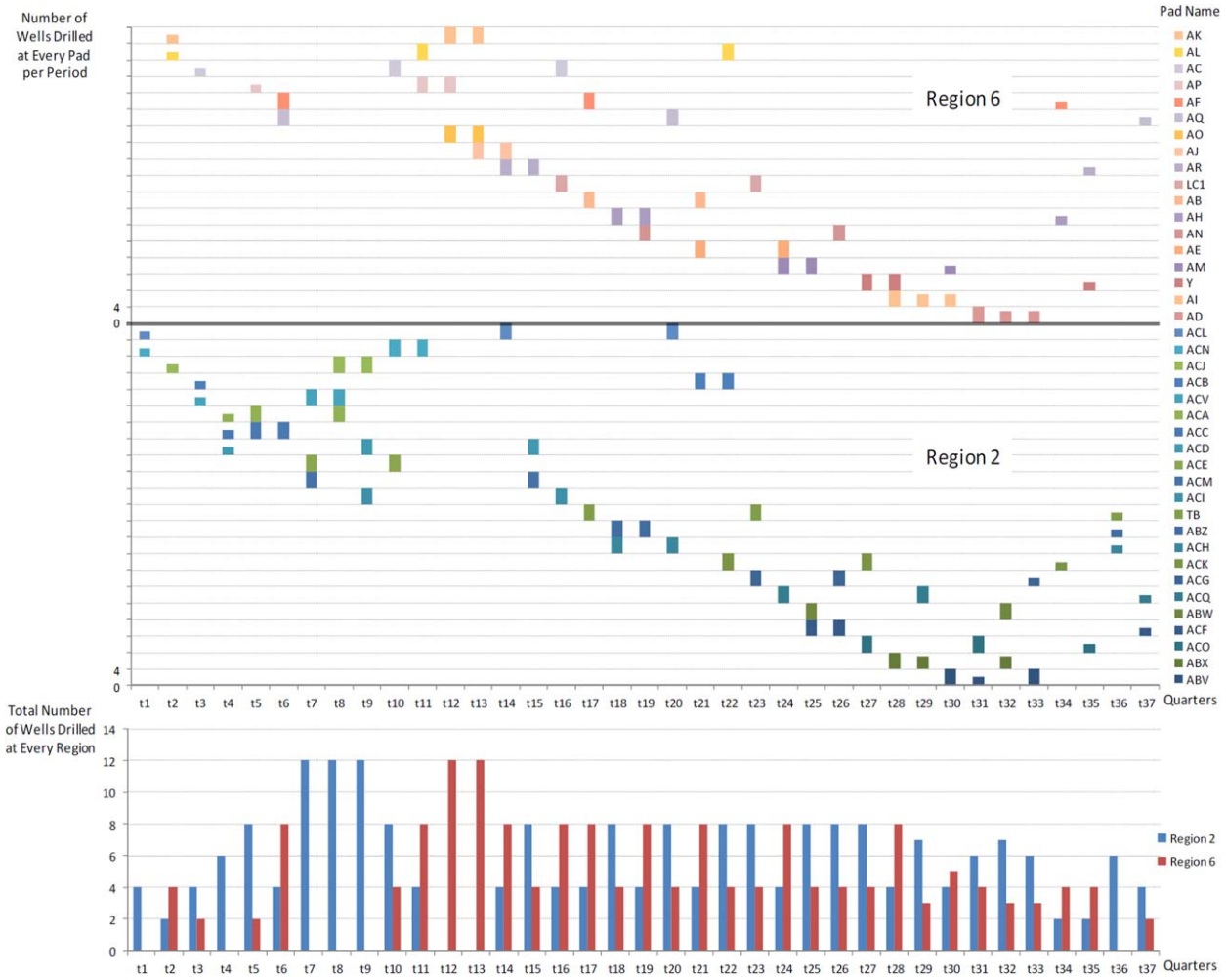

Figure 15. Optimal drilling strategy for the real-world case study.

[Color figure can be viewed in the online issue, which is available at wileyonlinelibrary.com.]

power of gas compressors; and the amount of freshwater used for well drilling and fracturing, transported from available reservoirs; so as to maximize the NPV of the project. All the problem conditions such as flow balances, equipment sizing and expansions are modeled in linear constraints, whereas concave terms arise in the objective function due to the economies of scale relations determining the cost of plants, pipelines, and compressors. Moreover, through a simple adaptation, the model can also account for shale gas composition variations depending on the geographic location of the wells.

As the model becomes intractable for commercial global optimizers, a two-level decomposition algorithm successively refining piecewise linear approximations of the concave cost terms and solving reduced MINLP problems was implemented. The use of the δ-piecewise linear formulation[30] yields good relaxations of the MILP models, whereas the logarithmic approximation recently proposed by Cafaro and Grossmann[29] avoids numerical difficulties in the execution of the nonglobal MINLP solver. The proposed BRO algorithm proves to be a useful tool for solving large-scale supply chain design problems in reasonable CPU times, although reducing the global optimality gap below 2.5% is quite hard for more challenging problems.

Results on realistic instances show the importance of heavier hydrocarbons to the economics of the project, and how the optimal planning of the drilling/fracturing strategy maximizes the utilization of gas processing/transportation infrastructure and improves the use of water resources. A real-world case study of the shale gas industry in northwestern Pennsylvania involving more than 150 potential sites for well-pads was successfully solved. The solution obtained is of particular importance for company decision-makers,

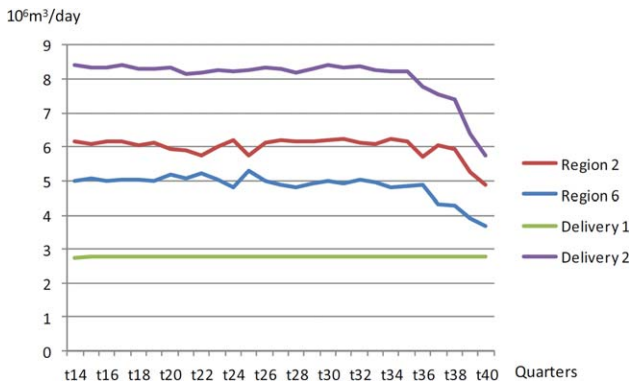

Figure 16. Shale gas flows in the optimal solution of the real-world case study.

[Color figure can be viewed in the online issue, which is available at wileyonlinelibrary.com.]

who cannot readily optimize the drilling strategy together with the pipeline configuration and compressor sizing so as to obtain a higher profit.

Future work will focus on the optimization of the gas pipeline pressures, as well as the consideration of stochastic conditions for products demands, gas prices, water availability, and shale gas production profiles at the wells.

Acknowledgments

Financial support from Fulbright Commission Argentina, CONICET and CAPD at Carnegie Mellon University is gratefully acknowledged. The authors are also most grateful to EQT Corporation for the case study provided to us.

Notation

Sets

F = freshwater sources
I = well-pads
J = junction nodes
K = gas demand points
P = gas processing and fractionation plants
L = ethane demand points
T = time periods

Parameters

dr = annual discount rate
$\text{ethdem}_{k,t}$ = maximum demand for ethane at node k in period t
ethp_t = unit price of ethane in period t (forecast)
fix_f = unit cost for freshwater acquisition from source f
$\text{fwa}_{f,t}$ = amount of freshwater available from source f during period t
$\text{gasdem}_{k,t}$ = maximum demand for methane at node k in period t
gasp_t = unit price of methane in period t (forecast)
gc_i, ec_i, lc_i = methane, ethane and LPG composition of the shale gas produced in pad i
$kr_{i,a}$ = value of a shale gas well of age a in pad i
ks, kd, kp, kc = Base cost of plants, wells, pipelines, and compressors in economy of scale functions
$l_{i,j}$ = distance between nodes i and j
lpgp_t = average unit price of LPGs in period t (forecast)
nd_t = number of days in time period t
$\hat{n}_i$ = upper bound on the number of wells to drill in pad i during one period
$\check{N}_i$ = upper bound on the number of wells to drill in pad i over the planning horizon
$\text{pw}_{i,a}$ = daily shale gas production of a well of age a (periods) drilled in pad i
rf_i = water reuse factor in well-pad i
sepmax = upper bound on the shale gas processing capacity of a single plant
s_g = gas density in standard conditions
shgp_t = unit cost of shale gas in period t
var_f = unit cost for freshwater transportation from source f
wr_i = amount of water required to drill and fracture a single well in pad i
τs, τp, τc = lead times for installing gas plants, pipelines, and compressors, in quarters

Binary variables

w_p = 1 if the processing plant p is operative during the planning horizon
$y_{i,n,t}$ = 1 if n wells are drilled at pad i during period t

Continuous variables

$\text{DFP}_{i,j,t}$ = diameter of the gas pipeline installed between i and j in period t to the power of 2.667
$\text{DGP}_{j,p,t}$ = diameter of the gas pipeline installed between j and p in period t to the power of 2.667
$\text{DTP}_{p,k,t}$ = diameter of the gas pipeline installed between p and k in period t to the power of 2.667
$\text{DLP}_{p,l,t}$ = diameter of the liquid pipeline installed between p and l in period t to the power of 2
$\text{EComp}_{j,t}$ = ethane composition of the shale gas flow at the outlet of node j during period t
$\text{FP}_{i,j,t}$ = shale gas flow from well-pad i to junction j during period t
$\text{FP}^{\text{E}}_{i,j,t}$ = individual ethane gas flow from well-pad i to junction j during period t
$\text{FP}^{\text{G}}_{i,j,t}$ = individual methane flow from well-pad i to junction j during period t
$\text{FP}^{\text{L}}_{i,j,t}$ = individual LPG flow from well-pad i to junction j during period t
$\text{FPCap}_{i,j,t}$ = total shale gas transportation capacity between i and j in period t
$\text{FPFlow}_{i,j,t}$ = shale gas transportation capacity installed between i and j in period t
$\text{GComp}_{j,t}$ = methane composition of the shale gas flow at the outlet of node j during period t
$\text{GP}_{j,p,t}$ = shale gas flow from junction node j to plant p during period t
$\text{GPCap}_{j,p,t}$ = total shale gas transportation capacity between j and p in period t
$\text{GPFlow}_{j,p,t}$ = shale gas transportation capacity installed between j and p in period t
$\text{JCInst}_{p,t}$ = compression power installed at node j in period t
$\text{JCP}_{p,t}$ = total compression power at j in period t
$\text{LComp}_{j,t}$ = LPG composition of the shale gas flow at the outlet of node j during period t
$\text{LP}_{p,l,t}$ = ethane flow from plant p to demand point l during period t
$\text{LPCap}_{p,l,t}$ = total ethane transportation capacity between p and l in period t
$\text{LPFlow}_{p,l,t}$ = ethane transportation capacity installed between p and l in period t
$N_{i,t}$ = number of wells drilled in pad i during period t
$\text{NP}_{p,t}$ = daily production of LPG in plant p during period t
$\text{PCInst}_{p,t}$ = compression power installed at plant p in period t
$\text{PCP}_{p,t}$ = total compression power at p in period t
$\text{TP}_{p,k,t}$ = dry gas (methane) flow from plant p to demand point k during period t
$\text{TPCap}_{p,k,t}$ = total methane transportation capacity between p and k in period t
$\text{TPFlow}_{p,k,t}$ = methane transportation capacity installed between p and k in period t
$\text{SepCap}_{p,t}$ = total shale gas processing capacity of plant p in period t
$\text{SepInst}_{p,t}$ = daily shale gas processing capacity installed in plant p at period t
$\text{SP}_{i,t}$ = daily shale gas production of well-pad i during period t
$\text{SP}^{\text{E}}_{i,t}$ = daily ethane production of well-pad i during period t
$\text{SP}^{\text{G}}_{i,t}$ = daily methane production of well-pad i during period t
$\text{SP}^{\text{L}}_{i,t}$ = daily LPG production of well-pad i during period t
$\text{WS}_{f,i,t}$ = amount of freshwater supplied from source f to pad i during period t

Literature Cited

1. U.S. Energy Information Administration (EIA). *U.S. 2012 Annual Energy Outlook with Projects to 2035*. Washington, DC: US Department of Energy, 2012.
2. U.S. Energy Information Administration (EIA). *Natural Gas Processing Plants in the United States: 2010 Update*. Washington, DC: US Department of Energy, 2011.
3. Laiglecia JI, Lopez-Negrete R, Diaz MS, Biegler LT. A simultaneous dynamic optimization approach for natural gas processing plants. *Proceedings of Foundations of Computer Aided Process Operations (FOCAPO)*. Savannah, GA, 2012.
4. Ladlee J, Jacquet J. *The Implications of Multi-Well Pads in the Marcellus Shale. Research & Policy Brief Series*. Ithaca, NY: Cornell University's Community & Regional Development Institute (CaRDI), 2011.
5. Stark M, Allingham R, Calder J, Lennartz-Walker T, Wai K, Thompson P, Zhao S. *Water and Shale Gas Development. Leveraging the US Experience in New Shale Developments*. Dublin, Ireland: Accenture, 2012.
6. Geoffrion AM, Graves GW. Multicommodity distribution system design by Benders decomposition. *Manag Sci*. 1974;20:822–844.
7. Melo MT, Nickel S, Saldanha-da-Gama F. Facility location and supply chain management—a review. *Eur J Oper Res*. 2009;196:401–412.

8. Durán MA, Grossmann IE. A mixed-integer nonlinear programming algorithm for process systems synthesis. *AIChE J*. 1986;32:592–606.
9. Iyer RR, Grossmann IE, Vasantharajan S, Cullick AS. Optimal planning and scheduling of offshore oil field infrastructure investment and operations. *Ind Eng Chem Res*. 1998;37:1380–1397.
10. Van Den Heever SA, Grossmann IE. An iterative aggregation/disaggregation approach for the solution of a mixed-integer nonlinear oilfield infrastructure planning model. *Ind Eng Chem Res*. 2000;39:1955–1971.
11. Gupta V, Grossmann IE. An efficient multiperiod MINLP model for optimal planning of offshore oil and gas field infrastructure. *Ind Eng Chem Res*. 2012;51:6823–6840.
12. Rahman MM, Rahman MK, Rahman SS. An integrated model for multiobjective design optimization of hydraulic fracturing. *J Pet Sci Eng*. 2001;31:41–62.
13. Mauter MS, Palmer VR, Tang Y, Behrer RP. The Next Frontier in United States Unconventional Shale Gas and Tight Oil Extraction: Strategic Reduction of Environmental Impact. Belfer Center for Science and International Affairs, Harvard Kennedy School, March 2013.
14. Rahm BG, Riha SJ. Toward strategic management of shale gas development: regional, collective impacts on water resources. *Environ Sci Policy*. 2012;17:12–23.
15. Yang L, Grossmann IE. Superstructure-based shale play water management optimization. *2013 AIChE Meeting*. San Francisco, CA, 2013.
16. Nikolaou M. Computer-aided process engineering in oil and gas production. *Comput Chem Eng*. 2013;51:96–101.
17. Troner A. Natural gas liquids in the shale revolution. James A. Baker III Institute for Public Police Rice University. Houston, TX, 2013.
18. Grossmann IE. Enterprise-wide optimization: a new frontier in process systems engineering. *AIChE J*. 2005;51:1846–1857.
19. Oliveira F, Gupta V, Hamacher S, Grossmann IE. A Lagrangean decomposition approach for oil supply chain investment planning under uncertainty with risk considerations. *Comput Chem Eng*. 2013;50:184–195.
20. Patzek TW, Male F, Marder M. Gas production in the Barnett shale obeys a simple scaling theory. *Proc Natl Acad Sci USA*. 2013;110:19731–19736.
21. Weymouth TR. Problems in natural gas engineering. *ASME Trans*. 1942;34:185–234.
22. Nahmias S. *Production and Operations Analysis*. New York, NY: McGraw-Hill, 2009.
23. Biegler LT, Grossmann IE, Westerberg AW. *Systematic Methods of Chemical Process Design*. New Jersey: Prentice Hall, 1997.
24. Guthrie KM. Capital cost estimating. *Chem Eng*. 1969;76:114–142.
25. McCarl BA. *Expanded GAMS User Guide Version 23.6*. Washington, DC: GAMS Development Corporation, 2011.
26. Geoffrion AM. Objective function approximations in mathematical programming. *Math Prog*. 1977;13:23–37.
27. Bergamini ML, Aguirre P, Grossmann IE. Logic-based outer approximation for globally optimal synthesis of process networks. *Comput Chem Eng*. 2005;29:1914–1933.
28. Bergamini ML, Grossmann IE, Scenna N, Aguirre P. An improved piecewise outer-approximation algorithm for the global optimization of MINLP models involving concave and bilinear terms. *Comput Chem Eng*. 2008;32:477–493.
29. Cafaro DC, Grossmann IE. Alternate approximation of concave cost functions for process design and supply chain optimization problems. *Comput Chem Eng*. 2014;60:376–380.
30. Padberg M. Approximating separable nonlinear functions via mixed zero-one programs. *Oper Res Lett*. 2000;27:1–5.
31. You F, Grossmann IE. Stochastic inventory management for tactical process planning under uncertainties: MINLP model and algorithms. *AIChE J*. 2011;57:1250–1277.
32. You F, Grossmann IE. Integrated multiechelon supply chain design with inventories under uncertainty: MINLP models, computational strategies. *AIChE J*. 2010;56:419–440.

Appendix A: Pipeline Flow, Compressor Power, and Cost Calculations

Gas pipeline diameter, flow, and cost

Similar to Durán and Grossmann,[8] the head loss in a gas pipeline segment i-j with diameter $D_{i,j}$ (in m), either transporting raw gas or methane, is assumed to be given by the Weymouth[21] flow Eq. A1

$$D_{i,j}=l_{i,j}^{\alpha}\left(P_i^2-P_j^2\right)^{-\alpha}\left(B_{i,j}\right)^{\alpha} \tag{A1}$$

where

$$B_{i,j}=s_{\mathrm{g}}T\left[P_0/(0.375T_0)\right]^2\left(\mathrm{Flow}_{i,j}\right)^2 \tag{A2}$$

s_{g} is the gas density (0.729 kg/m^3 for shale gas, 0.554 kg/m^3 for methane) in standard conditions ($P_0 = 0.1013$ MPa; $T_0 = 288.9$ K). T is the average gas temperature, in this case fixed at 288.9 K, and $\alpha = 3/16$. The input and output pressures (P_i, P_j, in MPa) are assumed to be known (see Assumption 9 in Problem Description section) as well as the pipeline length $l_{i,j}$ (in km). By combining A1 and A2, the gas flow ($\mathrm{Flow}_{i,j}$ in 10^6 m^3/day) can be expressed by Eq. A3

$$\mathrm{Flow}_{i,j}=\left\{\left(P_i^2-P_j^2\right)/s_{\mathrm{g}}T\left[P_0/(0.375T_0)\right]^2\right\}^{1/2}l_{i,j}^{-1/2}D_{i,j}^{1/2\alpha} \tag{A3}$$

As a result, if the inlet and outlet pressures are given, the gas flow is a function of the pipeline diameter to the power of 2.667, as shown in Eq. A4

$$\mathrm{Flow}_{i,j}=k_{i,j}l_{i,j}^{-0.5}D_{i,j}^{2.667} \tag{A4}$$

If shale gas pipelines transport raw gas from 2.1 to 1.4 MPa, the value of $k_{i,j}$ is 115.35. If the diameter is given in inches, it turns to 0.006423. In turn, dry gas pipelines operating from 6.0 to 4.0 MPa show a value of $k_{i,j}$ equal to 378.06, or 0.02105 if the diameter is given in inches.

Finally, we use the economy of scale function A5 to determine the cost of the gas pipeline i-j

$$\mathrm{Cost}_{i,j}=kpl_{i,j}l_{i,j}D_{i,j}^{0.60} \tag{A5}$$

By substituting $D_{i,j}$ with the variable $\mathrm{DP}_{i,j}=D_{i,j}^{2.667}$, Eqs. A4 and A5 yield A6 and A7, which are the equations actually used in the MINLP model

$$\mathrm{Flow}_{i,j}=k_{i,j}l_{i,j}^{-0.5}\quad \mathrm{DP}_{i,j} \tag{A6}$$

$$\mathrm{Cost}_{i,j}=kpl_{i,j}l_{i,j}\quad \mathrm{DP}_{i,j}^{0.225} \tag{A7}$$

Liquid pipeline diameter, flow and cost

To calculate liquid flows in a pipeline p-l, a mean velocity (normally equal to $v^{\max} = 1.5$ m/s) is assumed. That yields Eq. A8

$$\mathrm{Flow}_{p,l}=86,400\pi/4v^{\max}\rho D_{p,l}^2 \tag{A8}$$

where $\mathrm{Flow}_{p,l}$ is given in ton/day, D (diameter) in meters, 86,400 is the total number of seconds per day the pipeline remains operative, and ρ is the liquid density, in ton/m^3 (0.546 ton/m^3 for liquid ethane).

Using the concave cost function given in A5, and substituting $D_{p,l}$ with the variable $\mathrm{DP}_{p,l}=D_{p,l}^2$ yield Eqs. A9 and A10, which are the equations finally used in the MINLP model

$$\mathrm{Flow}_{p,l}=k_{p,l}\quad \mathrm{DP}_{p,l} \tag{A9}$$

$$\mathrm{Cost}_{p,l}=kpl_{p,l}l_{p,l}\quad \mathrm{DP}_{p,l}^{0.3} \tag{A10}$$

Compression power

As the compressors are assumed to be adiabatic, the power requirement of a compressor installed at node j (CP_j in kW) can be calculated through Eq. A11[8]

$$F_j \mathrm{CP}_j = (\mathrm{Pd}_j/\mathrm{Ps}_j)^b - 1 \quad \text{(A11)}$$

where

$$F_j = [(\gamma-1)\eta/(4.0426T\gamma)]\mathrm{Flow}_j^{-1} \quad \text{(A12)}$$

$$b = z(\gamma-1)/\gamma \quad \text{(A13)}$$

z is the gas compressibility factor (by the ideal gas assumption, $z = 1$), γ is the heat capacity ratio (typically, $\gamma = 1.26$), η is the compressor efficiency, and T is the gas temperature at suction conditions ($T = 288.9$ K). Flow_j is given in 10^6 m^3/day. By Assumption 9 (see Problem Description section) the compression ratio ($\mathrm{Pd}_j/\mathrm{Ps}_j$) both at junction and plant compressors is given (usually equal to 1.5). Hence, combining A11–A13 yields Eq. A14, stating that the power requirement is linearly proportional to the gas flow (see Eqs. 27 and 28 of the MINLP model)

$$\mathrm{CP}_j = [(4.0426T\gamma)/(\gamma-1)\eta][(\mathrm{Pd}_j/\mathrm{Ps}_j)^{z(\gamma-1)/\gamma} - 1]\mathrm{Flow}_j = kc_j\mathrm{Flow}_j \quad \text{(A14)}$$

Appendix B: Other Model Capabilities

Delayed production of a well

Some companies may often drill, fracture, and complete a nonconventional gas well, but the production of the well is delayed until the required infrastructure (pipelines, compressors and so forth) becomes available. In that case, the model is adapted by incorporating an integer variable accounting for the number of wells of pad i that become productive at the beginning of period t ($\mathrm{NP}_{i,t}$). Then Eq. B1 is added to the formulation, and Eq. 4 in the original model is replaced by B2

$$\sum_{\tau \le t} \mathrm{NP}_{i,\tau} \le \sum_{\tau < t} N_{i,\tau} \quad \forall i \in I, t \in T \quad \text{(B1)}$$

$$\sum_{\tau=1}^{t} \mathrm{NP}_{i,\tau}\mathrm{pw}_{i,t-\tau+1} = \mathrm{SP}_{i,t} \quad \forall i \in I, t > 1 \quad \text{(B2)}$$

Cost of rigs and crew for drilling new wells

If the cost of moving rigs, drilling crews, and other resources from one pad to the other is significant, the model should be able to determine the period in which the crew arrives at a pad to start or continue drilling new wells. With that purpose, we incorporate a new binary variable $x_{i,t}$ that is equal to one if at least one well is drilled and fractured in pad i during period t. That is controlled by Eqs. B3 and B4

$$N_{i,t} \le \check{N}_i x_{i,t} \quad \forall i \in I, t \in T \quad \text{(B3)}$$

$$N_{i,t} \ge x_{i,t} \quad \forall i \in I, t \in T \quad \text{(B4)}$$

As a result, the cost of arriving at a well-pad i to start or continue the drilling of new wells in period t is lower bounded by Eq. B5, and is included in the objective function 35

$$\mathrm{RC}_{i,t} \ge \mathrm{rig}\, c_i(x_{i,t} - x_{i,t-1}) \quad \forall i \in I, t \in T \quad \text{(B5)}$$

Finally, if the total number of rigs (and/or drilling crews) available is rigmax, Eq. B6 imposes an upper bound on the number of pads where new wells are drilled during a single period

$$\sum_{i \in I} x_{i,t} \le \mathrm{rigmax} \quad \forall t \in T \quad \text{(B6)}$$

Manuscript received Oct. 17, 2013, and revision received Jan. 28, 2014.